School of Mechanical Engineering
The University of Western Australia

# Sensor Selection and Testing for the Renewable Energy Vehicle

Travis Hydzik

October 2005

Supervisor: A/Professor James Trevelyan

Travis Hydzik
21 Tavistock Crescent
LYNWOOD WA 6147

14 October 2005

Professor Mark Bush
Dean
Faculty of Engineering, Computing and Mathematics
The University of Western Australia
35 Stirling Highway
CRAWLEY WA 6009

Dear Professor Bush

I take pleasure in submitting my thesis "Sensor Selection and Testing for the Renewable Energy Vehicle" as partial fulfilment of the requirements for the degree of Bachelor of Engineering (Mechatronics).

Yours sincerely

Travis Hydzik
10112111

# Abstract

The Renewable Energy Vehicle (REV) is a large University project that aims to demonstrate the viability of using renewable energy sources for transport. This project's aims were to select and test appropriate sensors for required measurements on the REV. The most common measurements; currents, voltages and temperatures were discussed as well as hydrogen concentration sensors needed due to safety reasons.

# Acknowledgements

It is with great pleasure I thank the following people who made this thesis possible.

**A/Professor James Trevelyan,** my Supervisor, for being approachable and for his extensive knowledge and help. It has been an incredible learning experience, which will benefit me immensely during my career.

**Rob Greenhalgh,** for all your advice on the safety aspects of my project.

**The REV Communications and Monitoring group,** for your helpful ideas and knowledge on electronic systems.

**The whole REV team** for making this project enjoyable and sociable.

**All my friends,** who have made my University experience very memorable. Thanks for all the good times.

**My family,** for the support and opportunities provided to me over the years. Thank you for your love and continuous encouragement.

# Contents

# List of Figures

# List of Tables

# List of Acronyms

DAQ Data Acquisition — the process by which events in the real world are translated into machine-readable signals.

EL Explosive Limit — the concentration at which an air and specific gas mixture becomes explosive.

EMI Electromagnetic Interference — the interference in signal transmission or reception caused by the radiation of electrical and magnetic fields.

FET Field Effect Transistor — a type of transistor commonly used for weak-signal amplification

JFET Junction Field Effect Transistor — the simplest type of field effect transistor

KISIS Knowledge based Intelligent system for the Selection of Industrial Sensors — a project developed by the Laboratory for Measurement and Instrumentation at the University of Twente to solve the sensor selection problem.

LSB Least Significant Bit — the smallest voltage change detectable by an A/D converter.

MOS Metal-Oxide Semiconductor (hydrogen concentration sensing type)

PCB Printed Circuit Board

PPE Personal Protective Equipment — the equipment and clothing required to lessen the risk of injury from or exposure to hazardous conditions

PPM Parts Per Million — a common unit of concentration of gases in air

REV Renewable Energy Vehicle — a project at The University of Western Australia that aims to demonstrate the viability of using renewable energy sources for transport.

RMS Root-Mean-Square

SAW Surface Acoustic Wave (hydrogen concentration sensing type)

STP Standard Temperature and Pressure — denotes an exact reference temperature of 0 °C (273.15 K) and pressure of 1 atm

SUC System Under Consideration

TC Temperature Coefficient — the relative change of a physical property when the temperature is changed by 1 K or 1 °C

TC Thermal Conductivity (hydrogen concentration sensing type)

# Chapter 1

# Introduction

The Renewable Energy Vehicle is a large University project that aims to demonstrate the viability of using renewable energy sources for transport. The aims of this final year thesis were to choose appropriate sensors for a selection of required physical quantities that needed to be measured, and to test that they would work as expected when finally installed in the vehicle.

## 1.1 Thesis overview

This thesis can be summarised as follows:

**Chapters 2 and 3** — Provides a background on the University's Renewable Energy Vehicle project and the process of sensor selection and testing in general.

**Chapters 4, 5 and 6** — Details the selection and testing process of three main measurements; hydrogen, electrical and temperature respectively.

**Chapter 7** — Provides some conclusions and outlines areas of further work.

# Chapter 2

# Background

This section gives a brief background on The University of Western Australia's Renewable Energy Vehicle project and the part sensors play.

## 2.1 The Renewable Energy Vehicle project

The Renewable Energy Vehicle (REV) project is a major University project that aims to design and construct a vehicle solely powered by a hybrid hydrogen fuel cell and solar panel system. The vehicle will accommodate two persons, resembling the cars of today, while still being low in weight and highly aerodynamic. Once design and construction is complete, the REV will be driven around Australia to demonstrate the viability of using renewable energy for personal transport.

## 2.2 Sensors

A sensor is a device that measures a physical quantity and outputs this as more useful information; the most common output is an electrical signal.

The physical quantities that needed to be measured on the REV were determined from the following requirements:

**Driver display** — Information displayed when one is driving the REV e.g. cabin temperatures and vehicle speed.

**Data logging** — Recording a measurand over a period of time, to be analysed at a later date e.g. battery voltages and component temperatures.

**Control** — The measurand used in control of another system e.g. the electrical control system requires battery voltage measurements, in order to either use or recharge the batteries.

**Safety** — A component's properties constantly monitored for safety e.g. hydrogen leak detection and motor temperatures.

A list of the measurements required in the REV can be found in Appendix A. There are over 100 individual measurements (sensors) required. This number was too large for a single thesis, hence the measurements that were of interest were those that shared the most common measurement principles. These were the voltages, currents and temperatures and this accounted for over 70 % of the measurements. Finally, due to safety reasons, three hydrogen concentration sensors were given the highest priority.

## 2.3 Sensor selection

Sensor selection is the process of obtaining a suitable sensor for a desired measurement. Before selecting a sensor, it is important to obtain and consider all available information about the sensor's future applications.

The first consideration is the measuring principle. These are basic physics principles that can be used to measure the desired physical quantity. The measuring principle may be a constraint imposed by its future application. In other cases, this constraint may not exist and hence will result in a larger sensor selection range.

The final step is determining all the required sensor criteria and to choose a sensor that matches this criteria. The criteria can be broken into the following three main sections.

### 2.3.1 Performance specifications

Performance specifications refer to properties of the sensor's input and/or output. Typical factors include [3]:

**Range** — Difference between the maximum and minimum value of the sensed parameter

**Resolution** — The smallest change the sensor can differentiate

**Accuracy** — Difference between the measured value and the true value

**Repeatability** — Ability to reproduce repeatedly with a given accuracy

**Sensitivity** — Ratio of change in output to a unit change of the input

**Zero offset** — A nonzero output value for no input

**Linearity** — Percentage of deviation from the best-fit linear calibration curve

**Drift** — The variation of output from a reference value over a period of time with change in no input value

**Response time** — The time lag between the input change and output change

**Bandwidth** — Frequency at which the output magnitude drops by 3 dB

**Resonance** — One or more frequencies at which output magnitude peaks occur

**Deadband** — The range of input variation for which there is no output variation

**Signal-to-noise ratio** — Ratio between the magnitude of the signal and the noise

### 2.3.2 Operating conditions

Operating conditions include issues of electrical properties and environmental operating conditions.

#### 2.3.2.1 Electrical characteristics

Electrical characteristics include the type of power supply, the sensors' power consumption and the sensors' electrical output.

The REV power source is a DC voltage, hence this restricts the power supply of the sensors to that of a DC voltage. Most components on the REV use either 5 V or 12 V, so a sensor that uses one of these voltages is favourable. The power consumption of the sensors should be minimal, so that all available power is directed to the motors rather then being 'wasted' on components.

The electrical output of the sensors was a constraint of the data acquisition (DAQ) hardware. The designed DAQ hardware used components that operated on 5 V, hence the sensors' output needed to be an analogue 0–5 V DC voltage.

#### 2.3.2.2 Environmental conditions

Environmental conditions are criteria set by the future environment of the sensor. The REV is planned to be driven around Australia. Therefore, the components will be subjected to Australia's harsh climatic environment.

Climatic conditions include factors such as ambient temperature and humidity. In the past, Australia has experienced extreme minimum and maximum temperatures [4] of -23.0 °C and 53.1 °C respectively. Hence, the components must be able to operate at least within this range.

### 2.3.3 Cost constraints

The problem, however, is that it is extremely difficult to select a sensor that matches all the constraints, due to the cost and time involved in producing a highly customised sensor. The REV is solely funded through company sponsorship and hence has the restriction of a tight budget on purchased items. Price is the biggest constraint. Other constraints such as electrical and environmental conditions may need to be sacrificed hence, the need for sensor testing.

Given the constraints the sensor is chosen by either browsing sensor manufactures' data sheets or by simply inputting the criteria into a sensor database such as GlobalSpec [5].

## 2.4 Sensor testing

Sensor testing is performed to ensure that when a sensor is finally installed into the REV it will work as expected. Sensor testing, as mentioned above, is the result of constraints having to be sacrificed due to factors such as time and cost. Therefore, tests are performed to determine how the sensor operates at various conditions, and if the sensor does not meet original constraints the sensor needs to be modified to be suitable.

The similar conditions used when selecting a sensor i.e. performance specifications and operating conditions, are also used when testing a sensor. In order to test a sensor in specific conditions, a controlled environment needs to be created.

### 2.4.1 Sensor calibration

Sensor calibration is the most important test. To ensure that the sensor is calibrated correctly and the exact performance specifications are determined. Calibration testing can simply be generating a known voltage with a variable power supply and observing the sensor's output, or it can be more involved such as generating a known concentration of a particular gas.

### 2.4.2 Extreme operating conditions

Extreme operating conditions refers to harsher environmental conditions the sensor would need to operate in and this is undertaken as a safety precaution. The main concern was temperature, as this could vary the sensor's operation greatly. If the sensors cannot operate in these extreme temperature conditions, then the surrounding temperature will need to be controlled to accommodate the sensor e.g. cooling fans; their location and size of inlets/outlets.

### 2.4.3 Minimise sensor failure

Finally, included in sensor testing are the ways to improve sensor life and minimise the probability of sensor failure. This can be achieved by simply placing the sensor in an enclosure to protect the sensor physically and from EMI, or more involved such as how the sensor will be positioned and fixed in the REV to maximise the sensor's operation. This includes positioning the sensor away from noise sources and/or from heat sources.

# Chapter 3

# Literature survey

THERE is little available literature specifically on the selection of sensors for an automotive fuel cell application. There is information on some parts of this topic. Hence, it has been divided into the following sections.

## 3.1 General sensor selection

The Laboratory for Measurement and Instrumentation at the University of Twente [6] published a number of articles addressing the sensor selection problem. One of their projects, named KISIS (Knowledge based Intelligent system for the Selection of Industrial Sensors) [7], is the development of a computer program that assists a designer with the selection of sensors for a given measurement problem. Unfortunately, this project has not been updated since 2002 and the software is still unavailable to the public. However, an article [8] published by the same research group does define the sensor selection problem and goes into detail explaining the relation between the measurand and the measurement, which is useful if the sensors are to be designed.

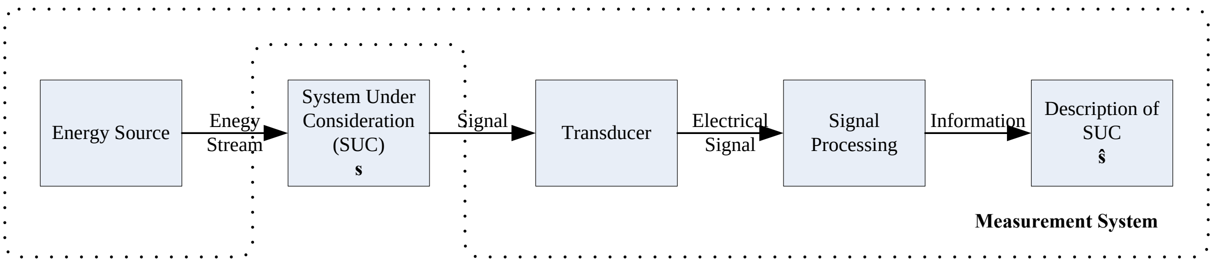


**Figure 3.1:** Sketch of a standard measurement system used when developing KISIS

Figure 3.1 shows the principle of a standard measurement system. The measurands are represented by the variable vector $s$ which is a parameter of the System Under Consideration (SUC). The object of the measurement system is to obtain an estimate of the variable $s$, which is defined as the variable $\hat{s}$. In order to obtain information from the SUC, there must be an exchange of energy. If the SUC radiates a form of energy, then a transducer can be used to convert this energy into electrical energy (an electrical signal). If the SUC does not radiate a form of energy, then an energy source must be provided.

The article "Selection of Sensors" [9] reproduced from "The Handbook of Measuring System Design" [10] is a free article on sensor selection that is available online. The article details the sensor selecting process and divides this into the following four main stages.

**Requirements** — An exhaustive list of information about the future applications, including all possible conditions of operation, environmental factors, and specifications with respect to quality, physical dimensions and costs.

**Selecting the measurement principles** — All measurement principles are considered and the optimum principle obtained through the basis of arguments.

**Selecting the sensing method** — Given a measurement process, a suitable sensing method is required. Again, all sensing methods are considered and the optimum selected.

**Sensor selection** — The final step is the selection of the sensor, which can be decided by looking at information published by manufacturers.

Though the article provides some good information about the process of sensor selection, including using the amount of fluid in a container as an example, it is only after having completed the sensor selection process with the constraints imposed by the REV that it is realised how irrelevant the above information is. The REV has a major cost constraint, hence this restricts the sensor selection range. The other major issue is time, the needed time to complete each stage of the selection process is not feasible, with over 100 individual sensors this will take a considerable amount of time. The article makes a good general point about sensor selection "Design methods have evolved over time, from purely intuitive to formal. The basic attitude is still the use of know-how contained in the minds of people and acquired through experience." After gaining experience with sensors, the author agrees with this statement.

## 3.2 Automotive sensors

There are a number of literary works that contain information about the sensors used in conventional petrol fuelled automobiles. The book “Understanding Automotive Electronics” [10] has a chapter on the sensors used in petrol fuelled vehicles, it makes an important statement about sensor selection “The sensors that are available to a control system designer are not always what the designer wants, because the ideal device may not be commercially available at acceptable costs”. This statement reiterates the need for sensor testing.

Similarly, the book titled “Automotive Computer Controlled Systems” [11] has a chapter on sensors, which gives a good understanding on how sensors in modern cars work. The book also stresses the topic of sensor diagnostics, discussing diagnostic techniques for the electrical parts of a car, including sensors.

A brief extract from “Bosch Technical Literature” [12] is on automotive sensors. It gives a basic understanding of the sensor problem specifically for an automotive application, as well as providing a list of sensors that would be found in current automobiles.

## 3.3 Fuel cell vehicles

A number of articles give a view of the sensors required in prototype vehicles that used fuel cells.

An article [13] published in the “International Journal of Hydrogen Energy” describes the design and construction of a fuel cell powered electrical vehicle very similar to the REV. The main difference was the choice of purchasing commercially available components rather than designing and constructing them. This included the chassis and the fuel cells. The article does not discuss the choice of sensors, but merely states what was needed. However, it gives some good statistics which may be useful in determining the capability of the REV.

One particular article [14] looks at the design and construction of a fuel cell powered electric bicycle. The design of the fuel cell power bicycle is quite simple when compared to the REV. However, the bicycle does have all major components of a fuel cell system including sensors. Actual provided test data including fuel cell efficiency and power-current and voltage-current curves may be useful in determining the future performance of the REV.

## 3.4 Measuring problem

"The Measurement, Instrumentation and Sensors Handbook" [15] addresses all issues of the measurement problem including sensor selection. In the initial chapters, the measurement problem is explained along with measurement accuracy and measurement standards. However, the most useful information is the in depth look at all the common physical quantity measuring systems including displacement, flows and electrical measurements. The amount of detail that is available for each different measurement system can be seen in the temperature chapter, where 11 different temperature measuring sensors are discussed. This book would be extremely helpful when selecting appropriate sensors for the measurements that have not yet been covered.

"The Mechatronics Handbook" [3] has a section on sensors. Similarly as the previous book, it looks at the most common measurement principles, but in lesser detail. The most useful information was its extensive selection criteria. This criteria was used when selecting the sensors' performance specifications for the sensors in this thesis.

The "Instrumentation Reference Book" [16] again addresses the general measuring problem, and hence is divided into instrumentation by application. Included in the book is a chapter titled "Instrumentation Systems" which provides another view on the measuring problem and sensor selection.

# Chapter 4

# Hydrogen

Hydrogen gas is extremely flammable having an EL of 4.1–74.8 % by volume in air. The minimum energy of hydrogen gas ignition in air at atmospheric pressure is about 0.02 mJ and it has been shown that escaped hydrogen is very easily ignited [17], the ignition temperature in air is 520–580 °C. In high concentrations, hydrogen may exclude an adequate supply of oxygen to the lungs, causing asphyxiation. Hydrogen gas is colourless, odourless and insipid, so the victim may be unaware of its presence. It is therefore crucial that any hydrogen leaks were detected quickly and accurately.

Hydrogen gas does react with oxygen to form water, though this reaction is extraordinarily slow at ambient temperature. At high temperatures or with an appropriate catalyst, hydrogen and oxygen gas are highly reactive. The hydrogen concentration in air at STP is 0.00005 %, but hydrogen emissions from lead acid batteries [18] and fossil fuel burning may result in higher levels. A hydrogen sensor needs to detect over the general level of ambient hydrogen levels (0.00005 %) and in a variety of environments. Hydrogen gas is the lightest element having a relative density[1] of 0.07. This means the gas is extremely buoyant and will accumulate near the ceiling of an airtight room. Three hydrogen gas sensors were needed; one general leak detector for the hydrogen testing workshop and two safety leak detectors in the driver's cabin and the fuel cell compartment of the REV.

## 4.1 Sensing types

There are a number of sensing principles used to detect hydrogen gas, the common sensing principles are Metal Oxide Semiconductor, Catalytic Bead, Thermal Conductivity,

[1]Relative density — the ratio between the density of hydrogen gas and that of dry air at STP

Electrochemical, and Acoustic Wave. Each have their advantages and disadvantages and these are discussed below.

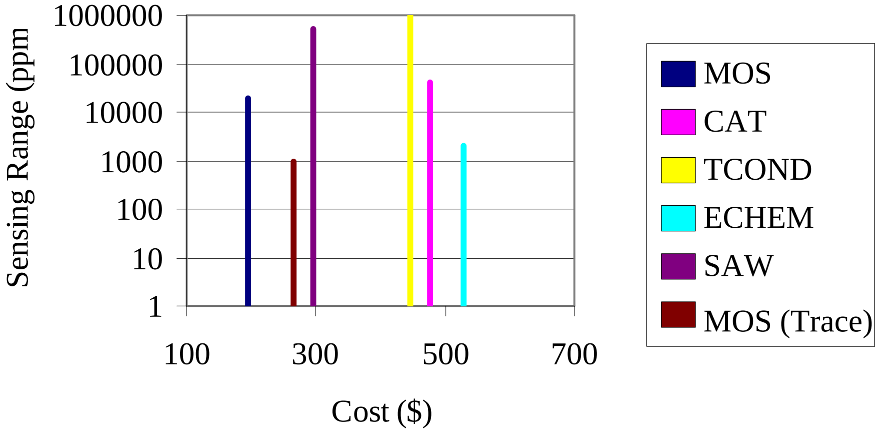


**Figure 4.1:** Sensing types and their approximate range and cost [1]

### 4.1.1 Metal-Oxide Semiconductor

Metal-oxide semiconductor (MOS) sensors are composed of a heater resistor to warm the sensor to its working temperature (between 200–500 °C [19]), and a sensitive resistor made of a metal-oxide layer deposited on the heater. The electrical resistance of the metal-oxide layer changes, depending on the temperature and the hydrogen content in the surrounding air. MOS sensors suffer from several problems including lack of selectivity, stability and sensitivity, and long response times [20].

### 4.1.2 Catalytic Bead

Catalytic bead sensors consist of two beads surrounding a wire operating at high temperatures (450 °C). One bead is passivated, so that it will not react when it comes into contact with hydrogen gas molecules, the other is coated with a catalyst to promote a reaction with the gas. The beads are generally placed on separate legs of a Wheatstone bridge circuit (Figure 4.2).

When hydrogen is present there is an increase in resistance on the catalysed bead and no change on the passivated bead. This changes the bridge balance and changes $V_{out}$.

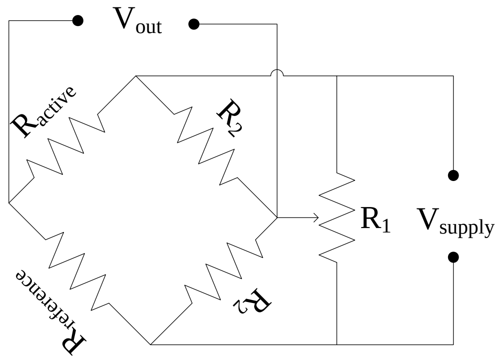


**Figure 4.2:** Wheatstone bridge circuit, $R_2$ keeps the bridge balanced, $R_1$ and $R_2$ are selected with relatively large resistance values

### 4.1.3 Thermal Conductivity

Thermal conductivity (TC) sensors are similar to catalytic bead sensors in that they compare the properties of a sample consisting of hydrogen in air to that of only air, which is used as a reference. TC sensors work by comparing the thermal conductivity of the sample to the reference. A heated thermistor is placed in the sample and another as a reference placed in the reference gas.

If the sample has a higher thermal conductivity than the reference, heat is lost from the exposed element and its temperature decreases, whilst if the thermal conductivity is lower than that of the reference, the temperature of the exposed element increases. Again, a Wheatstone bridge is used to measure the different resistance as a result of the temperature changes (Figure 4.2).

### 4.1.4 Electrochemical

Electrochemical sensors work on the same principle as fuel cells. They consist of an anode and cathode separated by a thin layer of electrolyte. When hydrogen passes over the electrolyte, a reversible chemical reaction occurs which generates a current, proportional to the gas concentration. Electrochemical sensors require very little power to operate, their power consumption is the lowest amongst all sensor types. Electrochemical sensors have high sensitivity, short reaction time, high reproducibility after calibration, linearity, zero point stability and relative low cross sensitivity. They are useful in safety and process control applications. One of the major drawbacks of electrochemical sensors is that the sensitivity decreases in the course of time, due to the loss of catalytic surface. [21].

### 4.1.5 Surface Acoustic Wave

Surface acoustic wave (SAW) sensors can be used in a number of applications, such as gas, fluid and biological sensing. SAW sensors work by creating an acoustic wave on two surfaces, with a piezoelectric transducer that propagates through the material, where it is then received by a second piezoelectric transducer that converts it back into an electrical signal. One surface is coated with a hydrogen reactive film that changes the properties of the material when hydrogen is present, the other surface is left uncoated and is used as a reference. This change in properties causes the received acoustic wave to change in frequency or amplitude, proportional to the concentration of hydrogen [22]. SAW sensors are reasonably priced, inherently rugged, very sensitive and intrinsically reliable [23]. SAW sensors have been successfully shown to measure hydrogen gas concentrations in an experimental setup [24][25].

## 4.2 Sensor Selection

When selecting a hydrogen sensor, the main factors are sensing range, resolution, operating conditions, and interference gasses. Depending on the sensing range, the data sheet can either specify the concentration in percent in volume or parts per million (PPM), where 1 % is equal to 10 000 PPM. After searching for sensors and obtaining quotes of $1350 and $3500, the company Neodym Technologies [1] was discovered that produced hydrogen sensors specifically for fuel cell applications at a low cost.

### 4.2.1 MiniKnowz

The MiniKnowz is Neodym Technologies' lowest priced combustible gas sensor between $68–106, depending on features, and was initially chosen for this reason (Figure 4.3). The MiniKnowz uses a MOS sensing element, that provides a typical response time of 4–10 s and a typical accuracy of ±800 PPM.

The distinct drawback of this sensor is that the sensor may be permanently damaged even by brief exposure to extremely high concentrations of hydrogen gas (typically >5 times the maximum sensing range) [26]. The sensors maximum sensing range is 20 000 PPM, meaning any concentrations greater then 10 % by volume in air, will cause damage. This level is not suitable for use in a hydrogen testing workshop where it is quite possible that these concentrations could occur. It is useful as a driver's cabin sensor

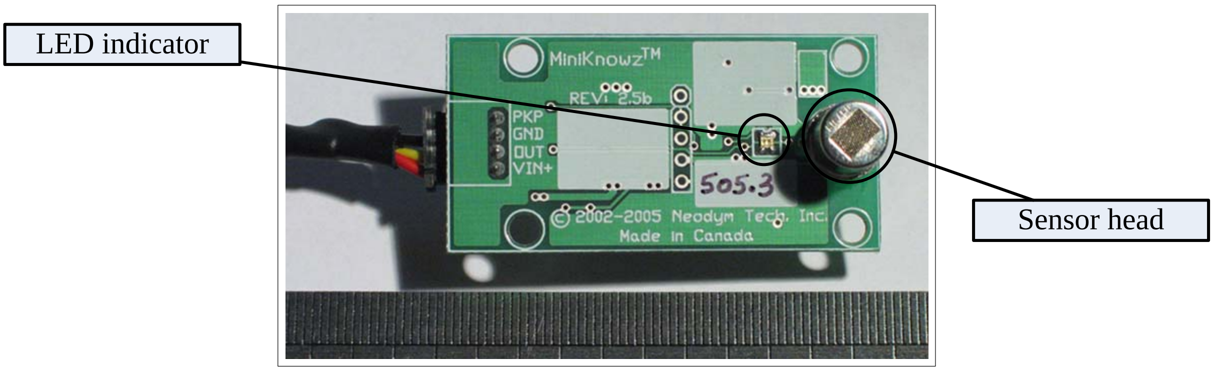


**Figure 4.3:** MiniKnowz hydrogen concentration sensor

where any hydrogen will be rare, and used only as a safety measure. Due to its inexpensive price, the MiniKnowz may be used as a disposable sensor. If a large leak occurred and the sensor was over exposed, it would go into its error state of 0 V, which is different from its normal working state of 0.5 V. The sensor would then either have to be replaced or the sensor head replaced and the sensor recalibrated.

Interference gas is another concern. Detectors will read accurately in the presence of homogeneous hydrogen gas/air mixtures, but will also produce readings in the presence of other inorganic and organic vapours. "Heterogeneous gas mixtures generally have a synergistic effect on the sensor, and in the absence of a target gas presence, the interference gases will manifest themselves as 'false' readings" [26]. The REV will be subject to various degrees of hydrocarbons from other vehicles exhaust. When emailed about this, Neodym Technologies stated "the sensor will pick up the unburnt hydrocarbons from gasoline engines if it is exposed to the direct exhaust stream. This has not been a problem for any of our automotive customers to date. Perhaps, because the inside of their fuel cell enclosures are positively ventilated" [27]. The sensor was tested to observe the effect of hydrocarbons.

### 4.2.2 Panterra

The Panterra is a range of gas sensors which use a variety of sensing technologies to sense a variety of gasses. The distinct advantage over the MiniKnowz is that they can operate in harsher environmental conditions, but this comes at a higher cost of approximately $325 per sensor, again depending on options.

The main advantage of the Panterra range is their ability to withstand high concentrations of hydrogen without permanent damage. This made them suitable as a general leak detector for use in the hydrogen testing workshop, where high hydrogen concentrations could occur. Initially, the Panterra-SONIC based on acoustic sensor technology was chosen due to its large sensing range of 0–100 % and inexpensive price, but was rejected after receiving a reply from Neodym Technologies stating "the sensor is still in beta and not ready for an automotive application" [27].

The choice of sensor came down to either the Panterra-CAT based on catalytic sensor technology or the Panterra-TCOND based on thermal conductivity sensor technology. The Panterra-TCOND has a sensing range of 0–100 % and the Panterra-CAT 0–40 000 PPM. The Panterra-TCOND has the advantage that the sensor can be operated in anaerobic and no-moisture environments, and are not affected by silicones [28], but due to its larger sensing range has a lower sensing resolution and accuracy when compared to the Panterra-CAT. It was decided that the Panterra-CAT was the most suitable option due to its high sensing resolution and accuracy, making it more useful detecting hydrogen concentrations up to the critical EL, where anything greater is considered dangerous (Figure 4.4).

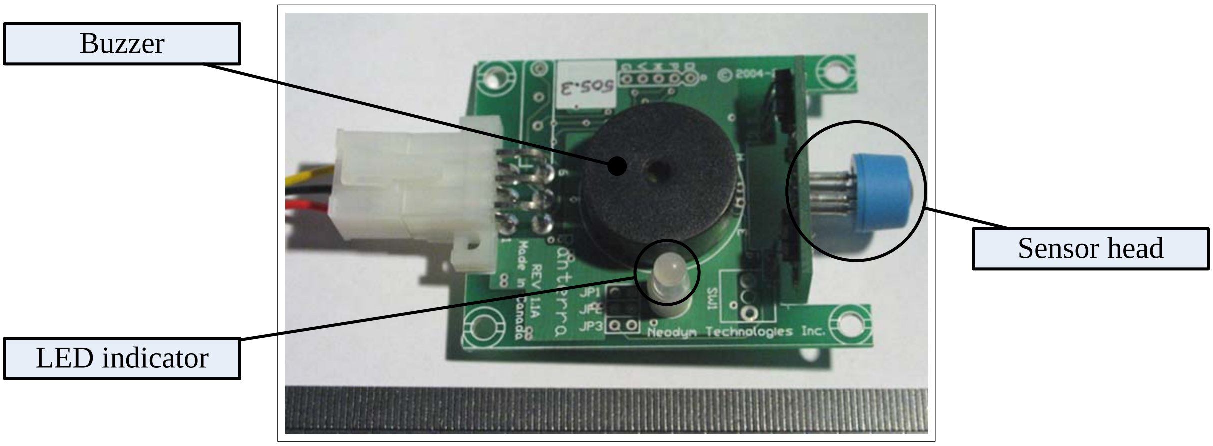


**Figure 4.4:** Panterra-CAT

## 4.3 Calibration Checking

The only method to check sensor accuracy and proper operation is via exposure of the sensor to a reference gas concentration, and to measure the sensor's output voltage. Neodym Technologies recommends that calibration checking should be performed as often as is practical, and no less frequently than once every six months [26].

Neodym Technologies' recommended method for generating calibration test gas mixtures is to dilute pure target gas with clean, normal air in a leak-free chamber of fixed, known volume [26]. The full safety procedure can be found in Appendix B. Six calibration tests were performed with each sensor type and the results can be seen in Appendix C.

To calculate the actual concentration of hydrogen gas in air, the volume of hydrogen in the syringe (specified in cubic centimeters) is divided by the container's volume (in mL) and then multiplied by 1 000 000. This gives a concentration in part per million. In the tests, a 1075±1 mL container was filled with a 5±0.05 cc syringe of 99.75±0.25 % (99.5 % minimum purity) hydrogen. This resulted in a concentration of 4640±63 PPM.

Given the sensor's output voltage ($V_{out}$), equation (4.1) was used to calculate the concentration.

$$Concentration = \frac{(V_{out} - V_{offset})Resolution}{StepSize} \tag{4.1}$$

where
$$\begin{aligned} Concentration &= \text{hydrogen concentration [PPM]} \\ V_{out} &= \text{output signal voltage [V]} \\ V_{offset} &= \text{zero offset voltage [V]} \\ StepSize &= \text{step voltage [V]} \\ Resolution &= \text{sensor resolution [PPM]} \end{aligned}$$

### 4.3.1 MiniKnowz

When observing the test results the obvious feature was the discrete step output, caused by the MiniKnowz's analogue to digital convertor, which has a resolution of 0.0784 V. The second feature was the randomness that the values settle at; the peak voltages range from 0.185±0.04–1.033±0.04 V and were a result of the air and hydrogen not mixing evenly. Using Figure C.1(c) as an example seen in Figure 4.5, the hydrogen concentration was calculated using the following values; $V_{out}$ = 1.025±0.04 V; $V_{offset}$ = 0.5 V; $StepSize$ = 0.080 V; $Resolution$ = 400 PPM.

As a result, a concentration of 2625±400 PPM was obtained. This value was lower than the supposed value of 4640±63 PPM, and could be attributed to the following experimental factors.

- The hydrogen and air was not proportionately mixed in the container creating pockets of high and low concentrations.
- Due to hydrogen being lighter than air, the hydrogen would always rise to the top of the container. If the sensor was placed in the middle of the container, inaccurate measurements would occur.

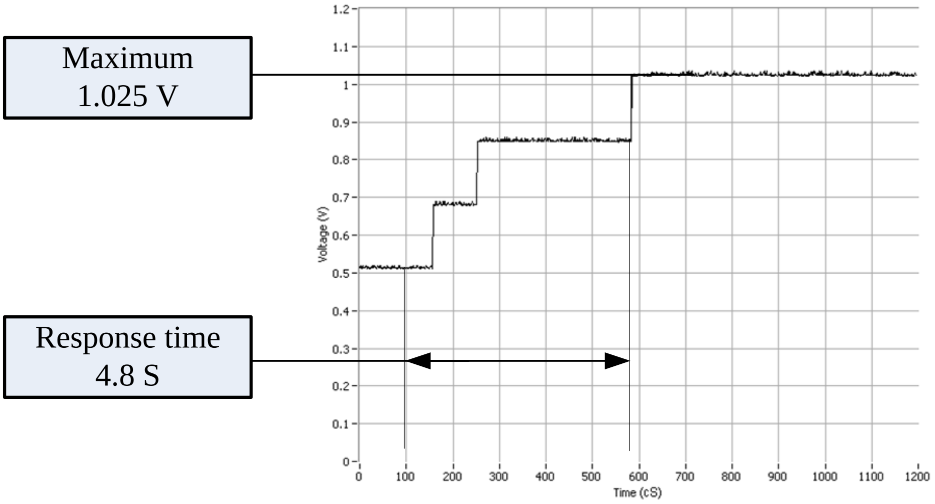


**Figure 4.5:** Example MiniKnowz test (Figure C.1(c))

- The transfer of hydrogen from the cylinder to the container was not 100 % efficient, air may have entered during any part of the transfer.
- The sensor may not have high accuracy. The MiniKnowz has a specified typical accuracy of ±800 PPM and a minimum accuracy of ±2000 PPM.

Neodym Technologies did give a manufacturer's certification of assembly, testing, and calibration with the sensor. It was therefore assumed that the sensor was calibrated correctly and it was any of the above factor(s) that caused the discrepancy.

Finally, by observing the sensor reading over time, an approximate response time was calculated. The syringe was emptied up to two seconds after the data acquisition logging was started. Hence, it took 4.8±1 s to detect the maximum concentration. This can be compared with the specified typical response time of 4 s and maximum response time of 10 s.

### 4.3.2 Panterra-CAT

Taking Figure C.2(e) as an example test result seen in Figure 4.6, the first noticeable feature was the smaller step sized when compared to the MiniKnowz, which resulted in a smoother curve. Again, a single test was used to determine the sensed concentration and response time. The hydrogen concentration was calculated using the following values; $V_{out} = 0.566{\pm}0.00245\,\text{V}$; $V_{offset} = 0.1\,\text{V}$; $StepSize = 0.0049\,\text{V}$; $Resolution = 40\,\text{PPM}$. As a result, a concentration of 3804±40 PPM was obtained. This was quite close to the actual concentration of 4640±63 PPM, and may have been due to the different sensing principle the Panterra-CAT uses that may measure low concentrations more accurately. Again, the same experimental factors as above could have contributed to the discrepancy. The Panterra-CAT has a specified typical accuracy of ±500 PPM and a minimum accuracy of ±1000 PPM.

Neodym technologies again provided a manufacturer's certification of assembly, testing, and calibration with the sensor.

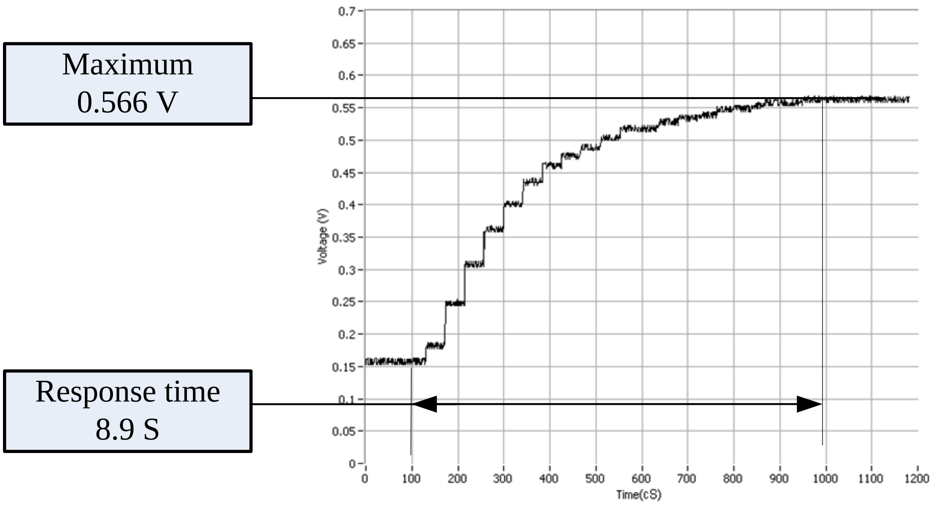


**Figure 4.6:** Example Panterra-CAT test (Figure C.2(e))

Finally, the response time was compared with the specifications. Again it was assumed that the syringe was approximately emptied up to two seconds after the data acquisition logging was started. By observing the test, a response time of 8.9±1 s was observed. This was comparable to the specified typical response time of 10 s and maximum response time of 20 s.

## 4.4 Cross Sensitivity

Cross-sensitivity refers to the response of a sensor to a gas other than hydrogen. The main interference gas of concern were the hydrocarbons in car exhaust.

The first test was to observe if car exhaust did cause 'false' readings. The same procedure was used as in Appendix B, except instead of injecting hydrogen gas, car exhaust was substituted.

Observing the test results found in Appendix C, it was evident that car exhaust did cause 'false' readings on both the MiniKnowz and Panterra-CAT. Using an example from each sensor type (Figure 4.7 and Figure 4.8), a maximum voltage of 0.68 V and 0.17 V was seen for the MiniKnowz and Panterra-CAT respectively. This equated to an incorrectly

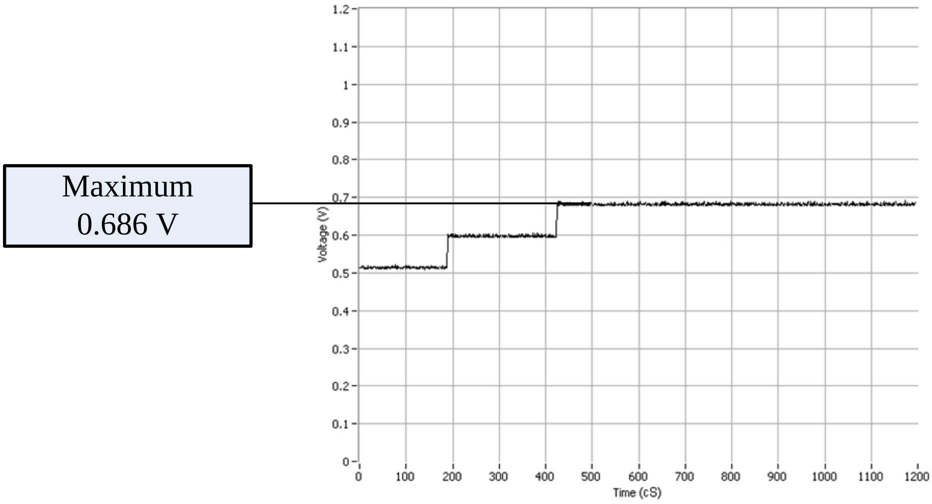


**Figure 4.7:** Example MiniKnowz test (Figure C.3(d))

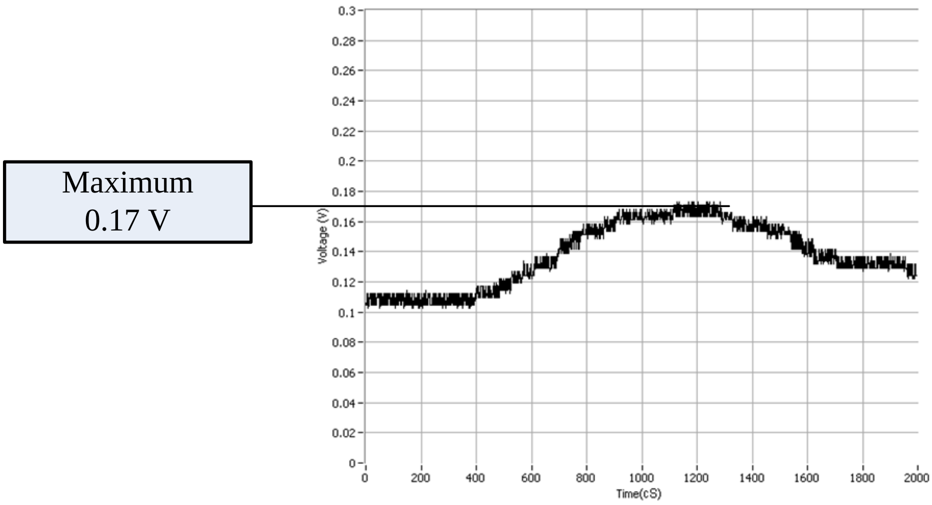


**Figure 4.8:** Example Panterra-CAT test (Figure C.4(d))

detected concentration of 900±400 PPM and 571±40 PPM respectively of sensed hydrogen gas. In conclusion the sensors did cause 'false' readings when exposed to car exhaust.

Finally, given that the sensors caused 'false' readings when exposed to car exhaust, it was needed to be determined if the sensors could still be used in the REV. The final test was to simulate the conditions that would be similar if the sensors were placed in the REV. The sensors were driven around during peak hours in a vehicle for 10 minutes. Two slightly different tests were conducted. One exposing the sensors directly to a stream of external air and one placing the sensor away from this stream of air simulating the actual position of the sensors in the REV.

In both tests the sensors were extremely close to their zero concentration offsets (Figure 4.9 and Figure 4.10). The largest voltage change was obtained from the Panterra-CAT when it was positioned close to the air stream, and this was a maximum

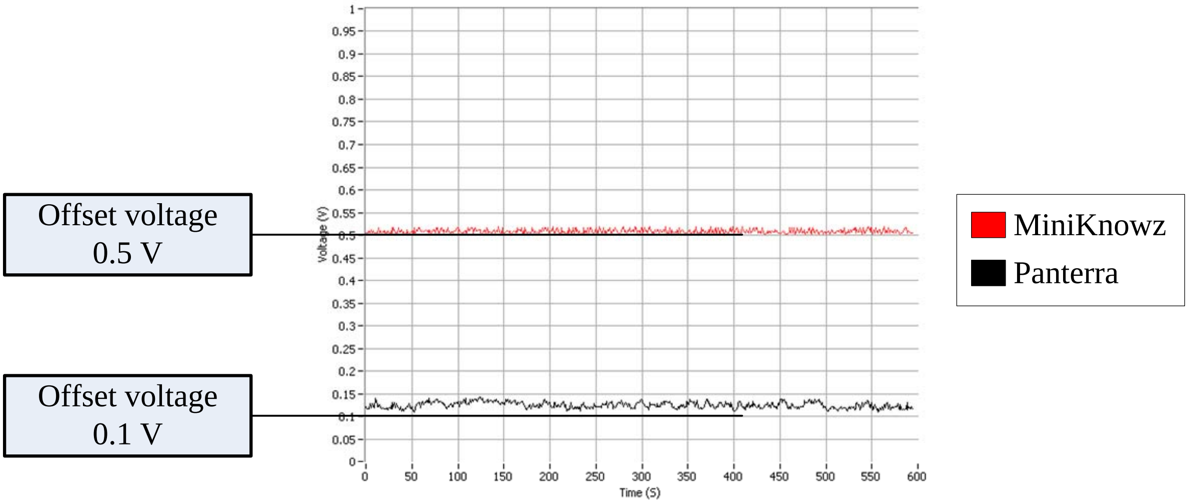


**Figure 4.9:** Hydrogen sensors positioned close to stream of air

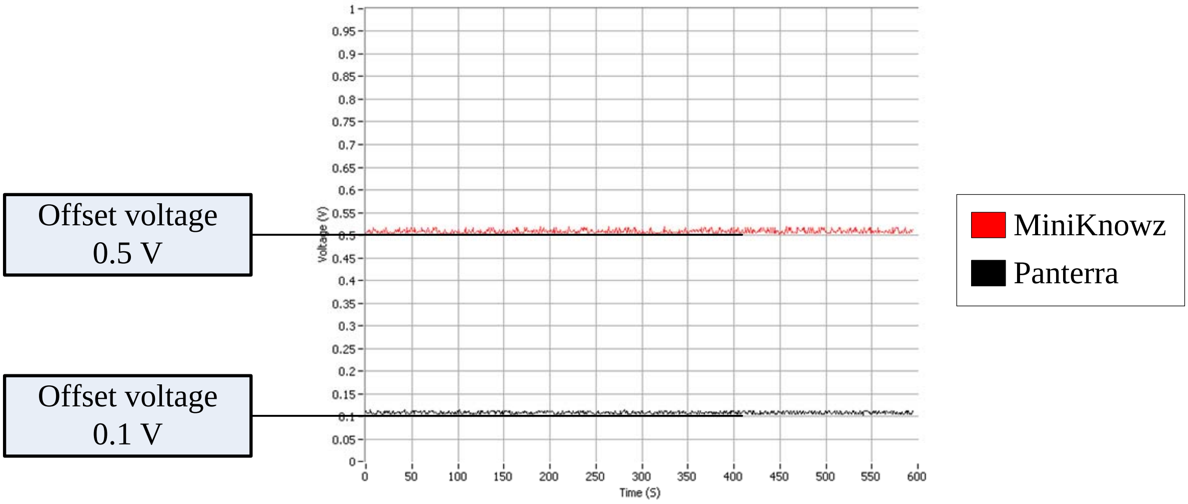


**Figure 4.10:** Away from air source

voltage of 0.143±0.00245 V and corresponded to a concentration of 350±40 PPM. When the sensors were positioned away from the air source, a maximum voltage of 0.114±0.00245 V was obtained, which corresponded to a concentration of 117±40 PPM which was insignificant. The slightly larger readings when placed next to the air stream, may have been a result of the air cooling the sensor head and causing incorrect readings. Also, the tests were conducted in a commercial petrol vehicle and the vehicle itself may have contributed to the sensors detecting hydrocarbons which would not be the case if it was situated in the REV.

However, due to the insignificance of the readings during both tests, the hydrogen concentration sensors are still suitable for use in the REV. If in fact it did cause a significant problem, the set voltage that determined a leak, would simply need to be set greater than the obtained maximum readings.

## 4.5 Increasing Reliability

There are a number of methods to improve the reliability of the hydrogen concentration sensors throughout their life. However, the most simple was placing the sensor in a metal enclosure and this protected the sensor from physical damage and from EMI. Three aluminium enclosures were purchased for the sensors. Slight modifications were made to the sensors' PCB to allow the sensors to fit tightly and holes were created in each enclosure to allow the sensors' head to be in contact with the surrounding air (Figure 4.11 and Figure 4.12).

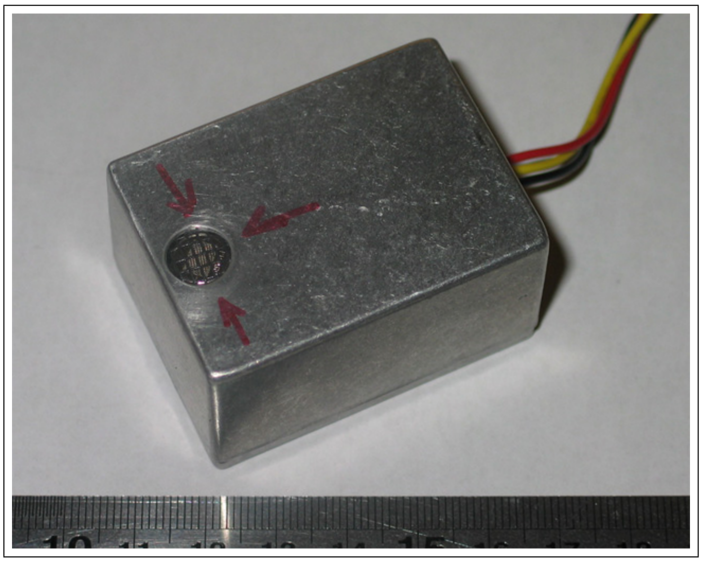

**Figure 4.11:** MiniKnowz in an aluminium enclosure

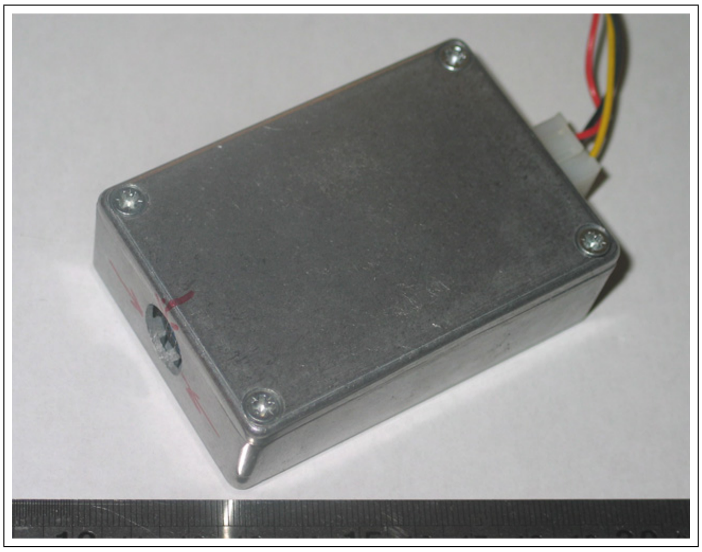

**Figure 4.12:** Panterra-CAT in an aluminium enclosure, the sensing hole is located on the side

In order for the sensors to operate free from error the sensors should be positioned correctly. Even though the REV design is still in its early stage, the approximate position of each sensor was determined. Hydrogen being lighter than air will accumulate at the highest possible position, usually the roof or apex. Therefore, the Panterra-CAT will be located on the roof of the hydrogen testing workshop, one MiniKnowz will be located above the fuel cell in the roof of the fuel cell compartment and the final MiniKnowz will be located at the apex in the driver's cabin (Figure 4.13). If the sensors were positioned at ground level, they may detect hydrogen gas as low concentrations as it passed. However, dangerous levels would accumulate at the roof, where it would remain undetected.

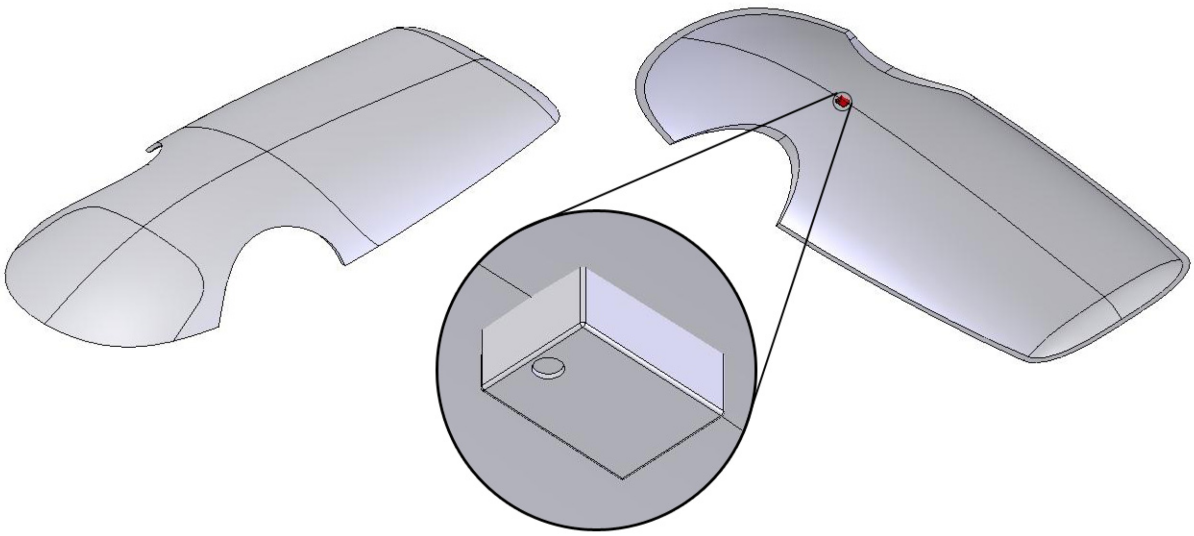

**Figure 4.13:** Approximate sensor placement of the MiniKnowz in the driver's cabin

Neodym Technologies recommends regularly cleaning the sensor head mesh of both the MiniKnowz and Panterra-CAT so that it is not obstructed by dust particles and debris. Cleaning the sensor head can be achieved with either compressed air or a soft nylon brush.

# Chapter 5

# Electrical

Electrical measurements include both currents and voltages and were required for data aquisition (DAQ) and for controlling the REV's electrical system. For this reason the measurements needed to have high accuracy and fast response times. All electrical measurements are already in an electrical signal form that DAQ hardware accepts. The signals, however, needed to be modified to be compatible with the specific DAQ hardware. This process is called signal conditioning and can include the processes of amplification, filtering, electrical isolation and multiplexing. The specifications of the DAQ hardware that was used is located in Appendix D.

## 5.1 Voltage

Most DAQ hardware have voltage input ranges of $\pm 10\,\mathrm{V}$ or $\pm 5\,\mathrm{V}$, so higher voltages cannot be measured directly as it will damage the hardware. Therefore, a voltage sensor was required to scale the voltage.

The voltages that were to be measured were all DC. This made selecting a suitable sensor easier. Voltage sensors can be self-powered or externally powered; with self-powered sensors being referred to as transducers. Most have isolated inputs/outputs which protects the DAQ hardware. The disadvantages with purchasing a voltage sensor was the lack of configurability with the input/output ranges. Also, most configurable sensors (convertors) are considerably expensive.

The cost efficient and more configurable sensor option was to design and build a custom voltage sensor using common components such as resistors and an operational amplifier (op-amp).

### 5.1.1 Voltage sensor design

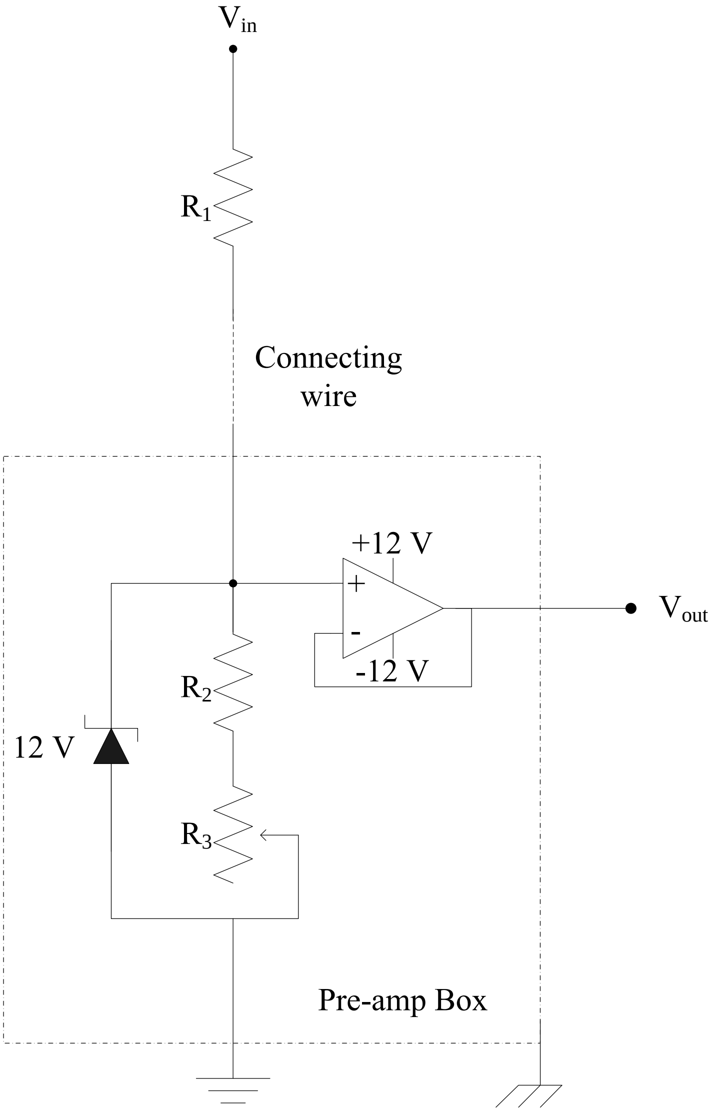


**Figure 5.1:** Basic voltage attenuator circuit

The basic circuit consisted of a voltage divider constructed using resistors (Figure 5.1). The divider scaled down the input voltage according to the resistor ratio found in equation (5.1). Where $R_3$ was used for fine adjustment.

$$V_{out} = V_{in}\frac{R_2}{R_1 + R_2} \tag{5.1}$$

A voltage follower (unity gain buffer) was placed on the output signal. A voltage follower with an ideal op-amp adheres to equation (5.2).

$$V_{out} = V_{in} \tag{5.2}$$

The input impedance of the op-amp is very high giving effective isolation of the output from the signal source. Very little power is drawn from the signal source avoiding loading effects [29]. According to National Instruments [30], it is important to select the proper components to maintain measurement accuracy and performance. Important considerations for selecting the op-amp included [31]:

- Clean power supply referenced to the analogue input ground
- Using a precision, low-noise op-amp with FET inputs for optimal performance
- The RMS noise added by the new circuitry should be less than the RMS noise of the DAQ device
- Offset Voltage Drift < 1 LSB/°C
- Equation (5.3) must hold

$$R_2 I_B < 1\,\text{LSB for desired gain} \tag{5.3}$$

where $R_2$ = source impedance [Ω]
$I_B$ = op-amp bias current [A]

The choice of the op-amp was the TL072C produced by STMicroelectronics [32] and was easily obtained. The TL072C is a low noise JFET input dual op-amp with a maximum input bios current ($I_B$) of 20 nA and a typical offset voltage drift of 10 $\mu$V/°C.

The DAQ hardware had an input of ±5 V with a resolution of 12 bits, where 1 LSB equated to 2.441±0.0005 mV. Given the LSB, the offset voltage drift of the op-amp (10 $\mu$V/°C) was compared with it and hence was significantly smaller. With the LSB and the input bios current, equation (5.3) was used to determine the maximum source impedance ($R_2$). This was calculated as 61±0.5 kΩ which was rounded down to the standard value of 56 kΩ.

To calculate the value of $R_3$, the resistors' tolerance ($T$) and difference between calculated and standardised values were taken into account.

$$\frac{R_2}{R_1 + R_2} = \frac{\acute{R_2}(1 \pm T) + R_3}{\acute{R_1}(1 \mp T) + \acute{R_2}(1 \pm T) + R_2} \tag{5.4}$$

Separating $R_3$,

$$R_3 = \frac{R_2 \acute{R}_1 (1 \mp T)}{R_1} - \acute{R}_2 (1 \pm T) \tag{5.5}$$

where $\acute{R}_1$ = standardised $R_1$ value [Ω]

$\acute{R}_2$ = standardised $R_2$ value [Ω]

$T$ = resistors' tolerance [%]

Using equation (5.1), $R_1$ was calculated depending on the voltage input. $R_3$ was a trimpot that allowed precise adjustments and was calculated using equation (5.5). The standardised values were chosen by rounding down to allow $R_3$ to compensate. If $R_3$ had an negative value, $R_2$ was needed to be dropped to the next lower standard value and then $R_3$ recalculated (Table 5.1).

**Table 5.1:** Examples of voltage range measurements required

| | | Calculated (kΩ) | | | | Standard (kΩ) | | |
|---|---|---|---|---|---|---|---|---|
| Voltage range (V) | Ratio | $R_1$ | $R_2$ | $R_{3,1}$ | $R_{3,2}$ | $R_1$ | $R_2$ | $R_3$ |
| 0 – 15 | 3:1 | 392 | 196 | 55 | 15 | 430 | 180 | 100 |
| 0 – 100 | 20:1 | 3724 | 196 | 45 | 6 | 3900 | 180 | 50 |
| 0 – 120 | 24:1 | 4508 | 196 | 44 | 5 | 4700 | 180 | 50 |

Finally, a 12 V zener diode was placed between the op-amp's input and ground, and this protected the op-amp and DAQ hardware in the event of any large voltage entering the circuit.

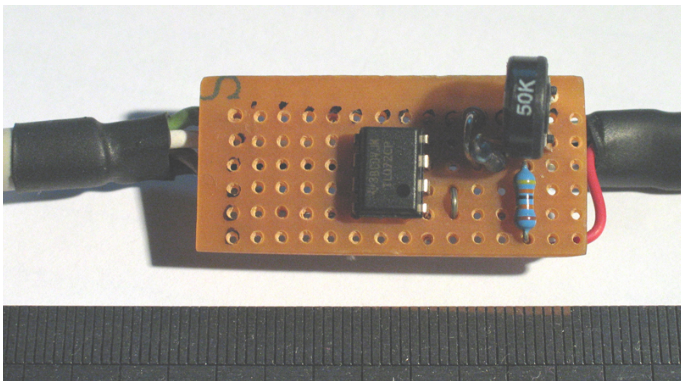


**Figure 5.2:** Constructed voltage sensor

### 5.1.2 Voltage sensor testing

To conduct tests on the voltage sensor two independent power sources were required. One to power the op-amp and one to provide an input voltage ($V_{in}$). A lab power supply was used to provide a variable voltage source between 0–15 V. Figure 5.2 shows a constructed voltage sensor.

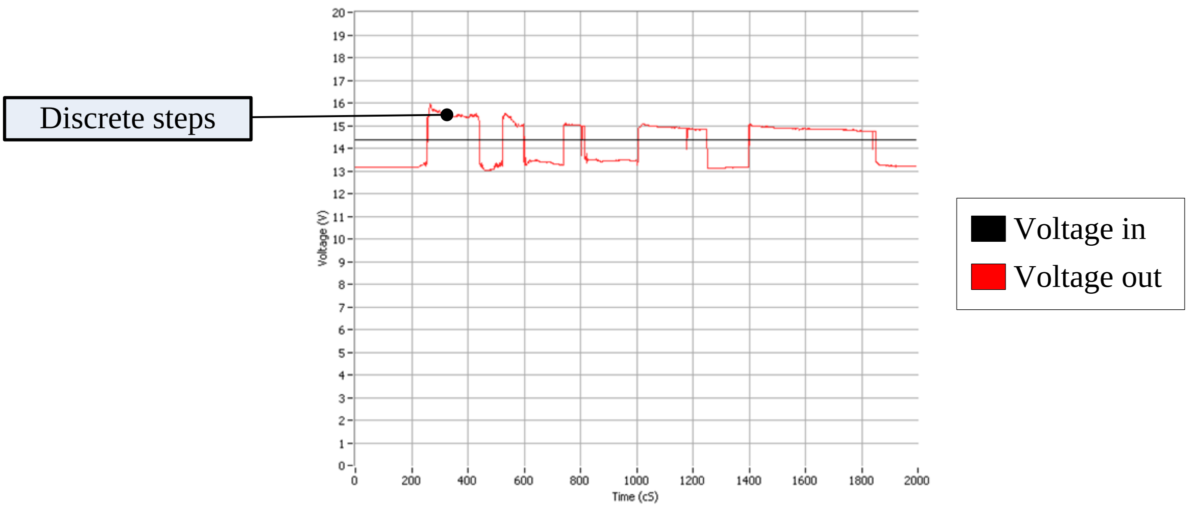


**Figure 5.3:** Voltage sensor calibration, discrete steps were caused when adjusting the trimpot

The initial test was calibration using the trimpot to ensure $V_{out}$ was precisely three times $V_{in}$ (Figure 5.3). It was very difficult to precisely adjust the trimpot as it was extremely sensitive and due to it having discrete resistance steps, it meant that it could not be adjusted to be exactly a third of the input voltage.

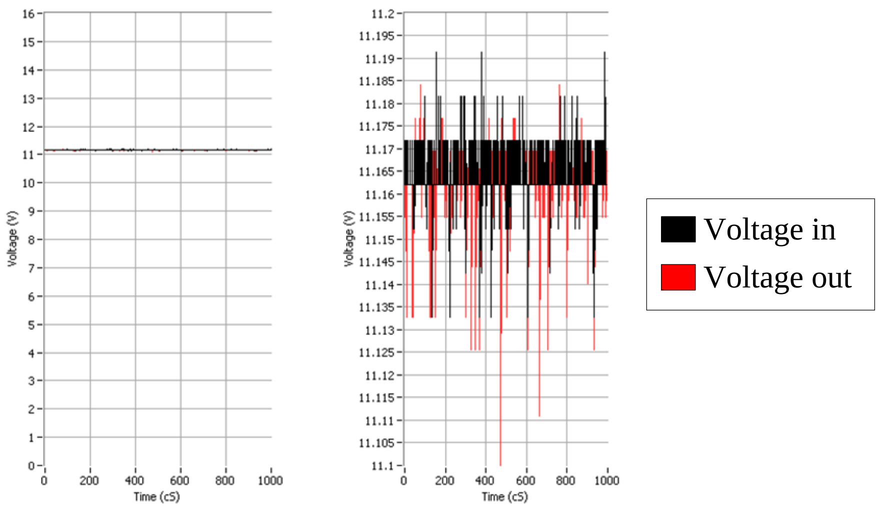


**Figure 5.4:** Precise voltage sensor calibration, the right is at higher resolution, enhancing the noise

Instead, a larger potentiometer was used to allow more precise adjustment. After precise adjustment, at a low resolution $V_{out}$ and $V_{in}$ were observed to be overlapping each other. At a higher resolution, noise was observed (Figure 5.4). This noise may have been generated from the power supply or was noise detected by the components. The trimpot and potentiometer may have contributed to the noise as well.

This potentiometer when precisely adjusted could then be replaced with a fixed resistor. In this case the value of the potentiometer was 33.2±0.22979 Ω and hence it could be seen why it was difficult to adjust the circuit using a 100 kΩ trimpot. Therefore, the trimpot could be used for large adjustments but a finer trimpot was needed for more precise adjustment. This, however, would have resulted in greater complexity in the sensor design. The other solution was to account for this difference in the software, but this would defeat the original idea of designing a circuit with $V_{out}$ and $V_{in}$ being an integer multiple ratio.

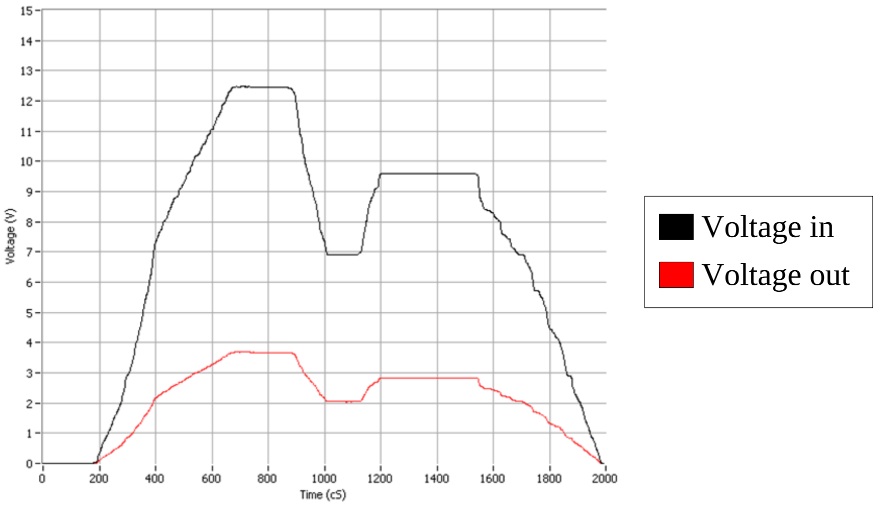


**Figure 5.5:** Voltage sensor test, $V_{in}$ manually varied while observing $V_{out}$

The second test was merely to observe if $V_{out}$ was a scaler of $V_{in}$ (Figure 5.5). $V_{in}$ was increased/decreased manually between the full range of 0–15 V and $V_{out}$ was observed to follow, confirming the sensor worked as expected. From observation, the sensor had no noticeable time delay.

One test done out of interest was to operate the sensor from a single power source ($V_{in}$). This had the benefits of operating as a self-powered sensor, without the need for the dual polarity power supply. In theory, it should have beeen possible as $V_{out}$ is never greater than $V_{in}$, but because of the op-amp requiring a negative power supply and the way the dual polarity power supply operated, it clearly could not operate as a self-powered unit (Figure 5.6). It would, however, work if $V_{out}$ was designed to have an offset voltage.

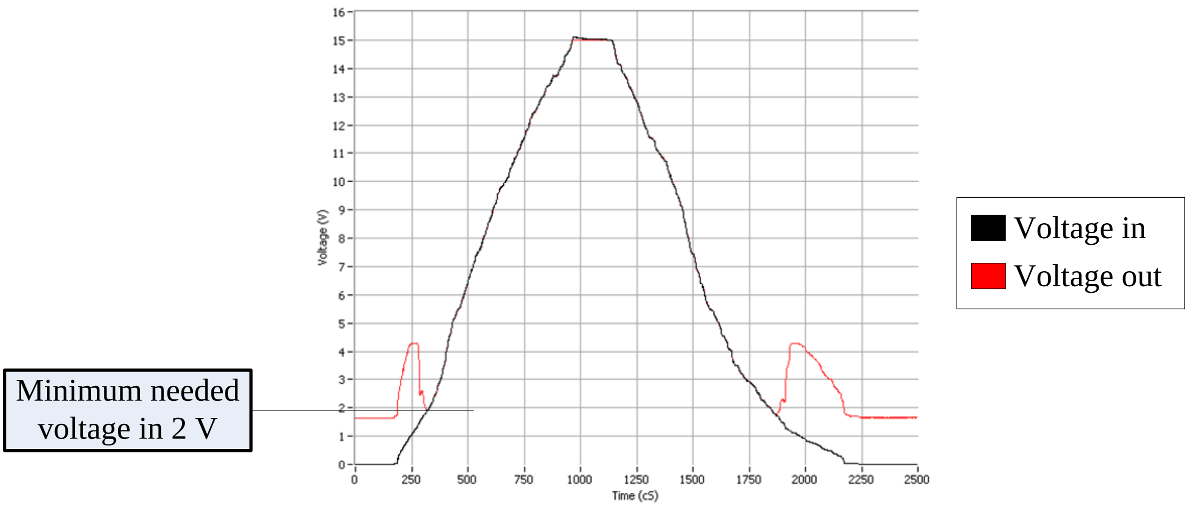


**Figure 5.6:** Voltage sensor self-powered test

## 5.2 Current

The easiest method of measuring current was to use a shunt resistor in series with the circuit. By measuring the voltage across the shunt resistor and knowing the resistor's value, the current was calculated using Ohm's Law. In order to minimise power loss from the circuit a very low resistor was used. This resulted in a very low voltage across the resistor which was too low to be measured with the DAQ hardware.

The second problem was voltages to the load may have been greater than 100 V. Since the DAQ hardware was grounded and most likely not isolated, 100 V would have been entering it which was above its maximum input voltage (20 V).

Again an amplifier was used to solve these two problems (Figure 5.7).

### 5.2.1 Current sensor design

Analog Devices [33] make the AD620 a low cost high accuracy instrumentation amplifier that requires only one external resistor to set gains of 1–1000 [34]. This allowed for configurability and a minimum voltage drop of 5 mV. Using Ohm's Law the required shunt resistances were determined (Table 5.2).

**Table 5.2:** Examples of current range measurements required

| Current range (A) | Maximum current (A) | $R_{shunt}$ (mΩ) |
|---|---|---|
| -2–4 | 4 | 1.25 |
| -2–5 | 5 | 1.00 |
| 0–7 | 7 | 0.72 |
| 0–20 | 20 | 0.25 |

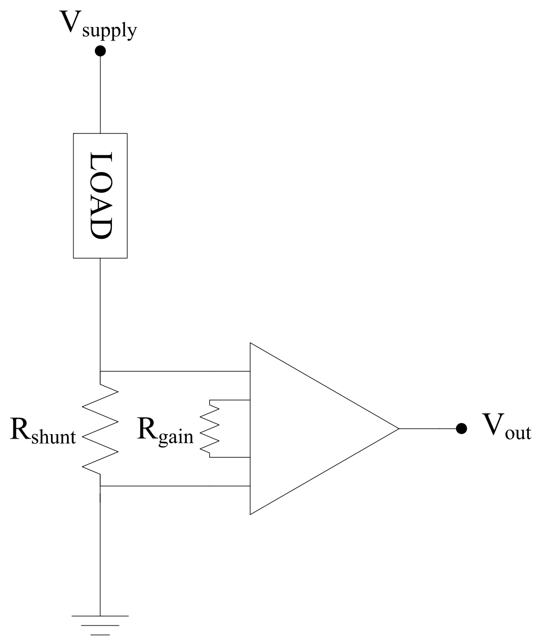


**Figure 5.7:** Current measurement circuit using a shunt resistor

The required resistances were so small that the wire used to transfer the power could actually be used as a shunt resistor.

### 5.2.2 Current sensor testing

To conduct tests, a circuit with a variable current was created. The lab power supply was capable of a maximum of 5 A, so the current sensor was designed for a current range of 0–5 A. A 4 Ω resistor was used as the load (Figure 5.8).

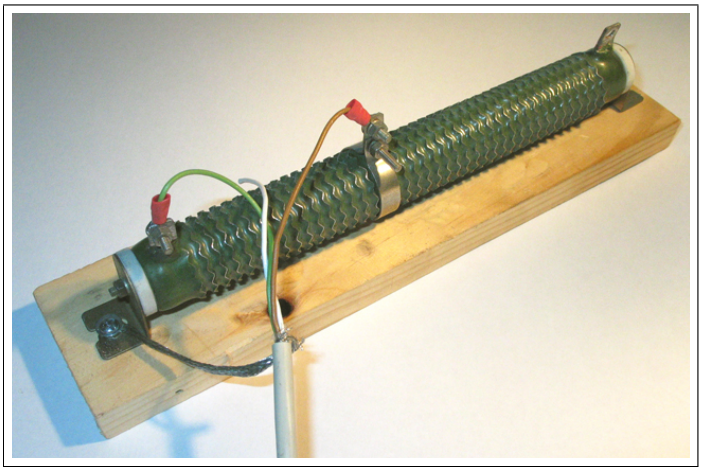

**Figure 5.8:** High power-rated resistor used as the load for current testing

Using Ohm's Law the voltage required to produce 5 A is 20 V, which the lab power supply was capable of. The power output (in this case 100 W) must be lower than the resistor's power rating, which it was. The wire used was flexible 0.75 mm$^2$ diameter copper wire, with a current rating of 7.5 A.

$$R = \frac{\rho L}{A} \tag{5.6}$$

Separating $L$,

$$L = \frac{RA}{\rho} \tag{5.7}$$

where $R$ = resistance of the wire [Ω] (1 mΩ)
$\rho$ = resistivity of copper [Ωm] (16.8 nΩm at 20 °C [35])
$L$ = required length of the wire [m]
$A$ = cross-section area [m$^2$] (0.75 mm$^2$)

Using equation (5.7) the length of wire required was calculated as 44.6±0.1 mm. Hence, signal cable was soldered to the current carrying cable at a distance of approximately 50±5 mm apart (Figure 5.9).

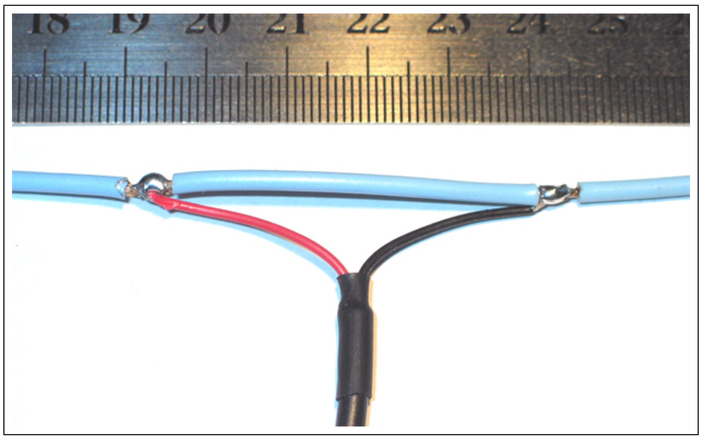

**Figure 5.9:** 50 mm non-shielded wire used as a current shunt

For initial testing the instrumentation amplifier was set to its maximum gain of approximately 1000, using equation (5.8). A 47.4±0.24266 Ω resistor was used to produce a gain of approximately 1040.

$$R_G = \frac{49.4k\Omega}{G-1} \tag{5.8}$$

where $R_G$ = gain programming resistor [Ω]
$G$ = instrumentation amplifier's gain

The initial tests showed $V_{out}$ was proportional to the current, but the signal was constantly alternating between the voltage signal and 0 V (Figure 5.11). It was thought

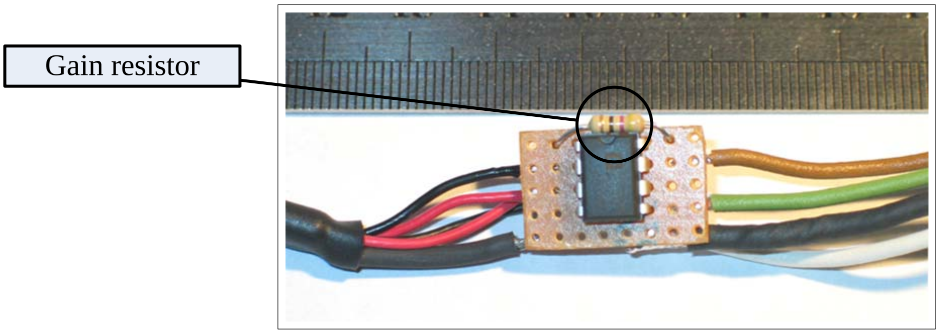


**Figure 5.10:** Constructed current sensor, resistor used to program gain shown

that due to amplification of an extremely small voltage (5 mV), any noise was amplified by a factor of approximately 1000 as well. For the next test, shielded cable was used and the method of joining the signal wire to the current carrying cable was modified.

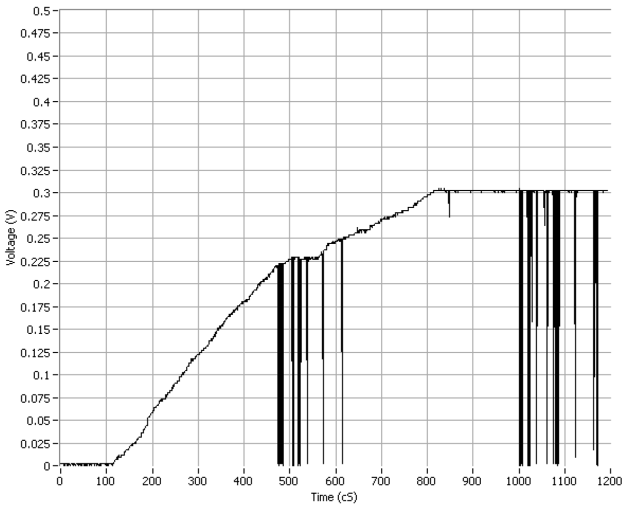


**Figure 5.11:** Current sensor test with non-shielded cable

When stripping the insulation from the 24-strand cable to connect the signal wires, it was extremely difficult not to damage the wires and hence increase the resistance. With the next test, any wires that may have been accidentally damaged were soldered first (Figure 5.12 and Figure 5.13).

The test produced some clean looking graphs that were proportional to current but after 15 s the same alternating signal developed (Figure 5.14).

In order to minimise the possibility of any added noise into the circuit, the dual polarity power supply which powered the instrumentation amplifier was combined with the current shunt circuit onto a single professionally printed PCB (Figure 5.15).

With this updated current sensor two independent tests were conducted. One using the previous 50 mm shielded cable and one using 200 mm non-shielded cable (Figure 5.16).

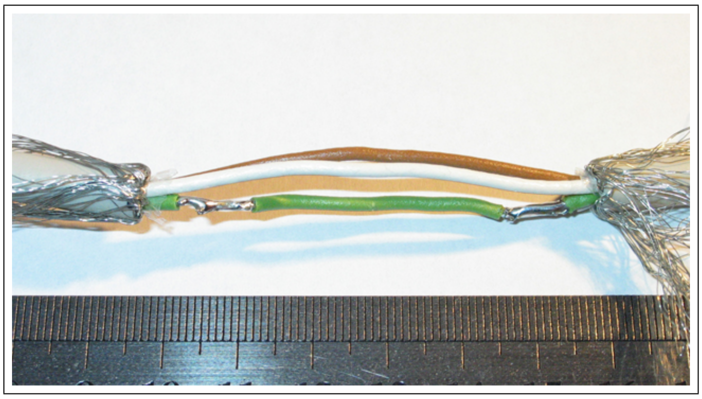

**Figure 5.12:** 50 mm shielded cable used as a current shunt soldered first

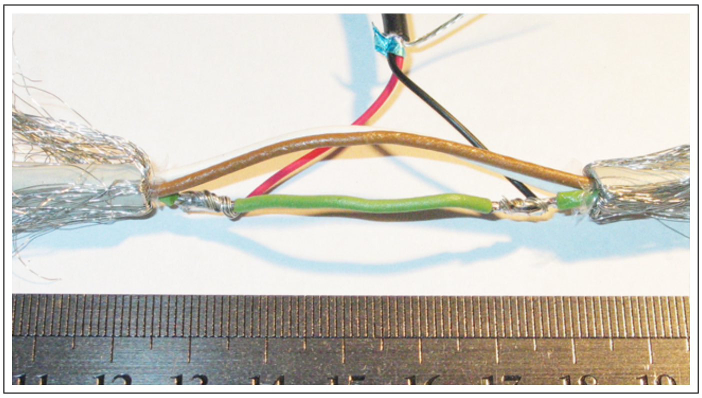

**Figure 5.13:** 50 mm shielded cable used as a current shunt with signal wires attached

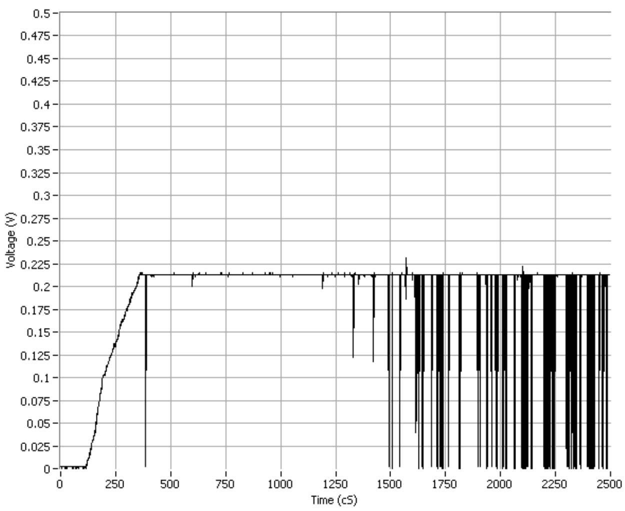


**Figure 5.14:** 50 mm current sensor test with shielded cable

The initial test was to observe if the noise could still be noticed in the circuit. The power supply was set at a constant voltage and current. The acquired voltage remained fairly constant with minor spikes occasionally occurring (Figure E.1 and Figure E.2). Hence, the updated current shunt had removed a significant amount of the alternating behaviour.

The second test was to observe if the voltage output was a multiple of the actual

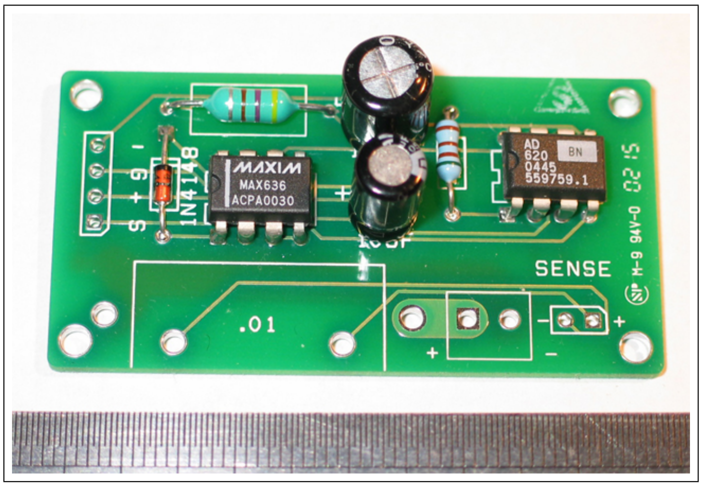


**Figure 5.15:** Combined dual polarity power supply and current shunt

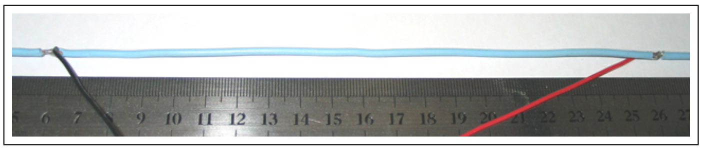

**Figure 5.16:** 200 mm non-shielded cable used as current shunt

current. The actual current was measured with a multimeter in parallel with the load circuit and the voltage out was measured using the DAQ hardware. The raw results are located in Appendix E. The data was plotted and a linear trendline added (Figure 5.17 and Figure 5.18).

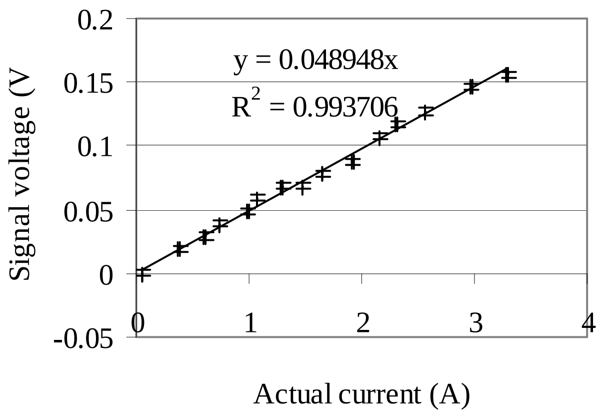


**Figure 5.17:** Current shunt test using 50 mm of shielded cable

It was observed that the two plots were quite linear with the 50 mm and 200 mm shunt having an $R^2$ value of 0.993706 and 0.999824 respectively. Determining the gradient of the two trendlines allowed the voltage-current ratio to be determined and it was 0.048948 and 0.249871 respectively. This multiplication factor will need to be implemented in

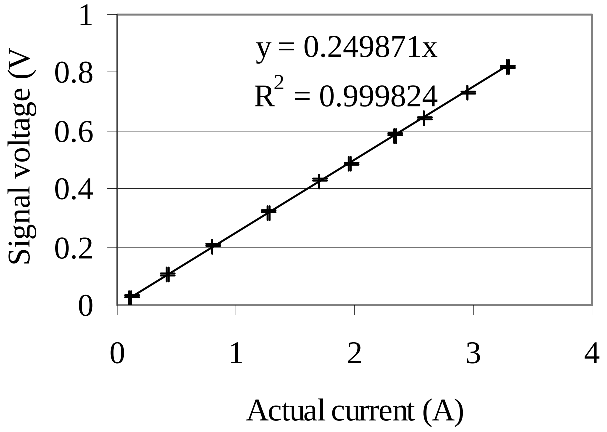


**Figure 5.18:** Current shunt test using 200 mm of non-shielded cable

software to convert from the voltage out to actual current. The linearity of each plot confirmed that the sensor was working as expected. The tests also showed that the initial calculated length of 50 mm that was assumed to equate to 1 mΩ was actually 48.948 1 μΩ, approximately 20 times lower. This was probably due to inaccuracies when measuring the shunt length, and the assumed wires' diameter may have varied. This very small resistance may also explain the previous readings when the signal was constantly alternating between $V_{out}$ and 0 V.

Measuring currents with a shunt resistor was a cost effective method that produced favourable results. However, problems did arrive when wire was used as the shunt resistor. If the wire was too short, the instrumentation amplifier measured an extremely small signal and hence noise interfered with the signal easily. When the wire was extended it acted as an antenna picking up EMI. This would be a greater problem if the current sensors were situated around the REV motors which produced large amounts of EMI. The alternative to using a wire as a shunt is to purchase specifically made shunt resistors, even though they have the disadvantage of being costly and relatively heavier. However, they can be designed to be a specific resistance and made to withstand temperature changes which is beneficial.

## 5.3 Dual polarity power supply

One of the problems with using an amplifier is the requirement of a dual polarity power supply. Usually, a simple dual polarity power supply can be made if an AC power source is available, but since the REV will be solely operating on DC power, an inverting DC-DC regulator circuit is required. MAXIM [36] produces the semiconductor MAX636 [37] which is an inverting switching regulator specifically designed for minimum component DC-DC conversion in the 5–500 mW range (Figure 5.19). Figure 5.20 shows the constructed dual polarity power supply.

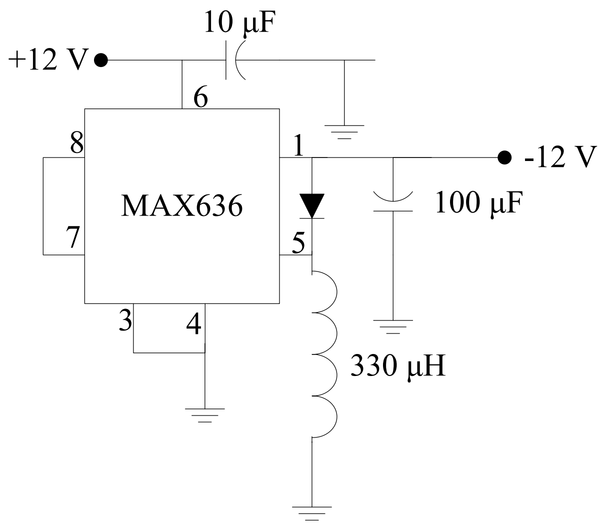


**Figure 5.19:** Inverting switching regulator based around the MAX636

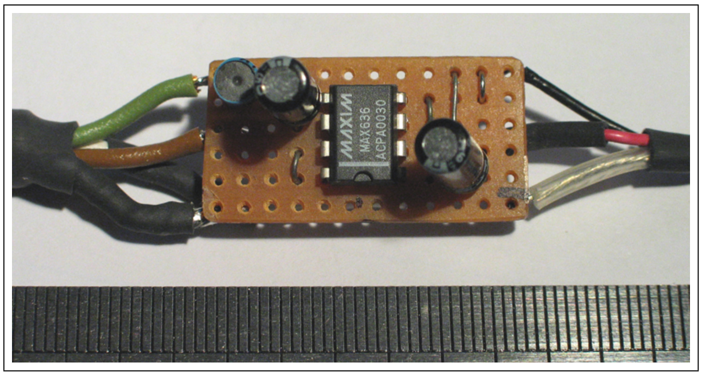


**Figure 5.20:** Constructed inverting switching regulator

### 5.3.1 Testing

The first test was to observe how the dual polarity power supply negative output changed depending on the received input. The input voltage was set at 0 V and the voltage gradually increased to approximately 12 V, which would be the expected voltage in normal operation. After being steady at approximately 12 V the power supply was gradually decreased back to 0 V (Figure 5.21). It was observed that 4.2 V was required for the dual polarity power supply to reach its minimum output of -11.7 V. At the dual polarity power supply's minimum, it was observed that the output created large oscillations when the input was at its max of 12 V.

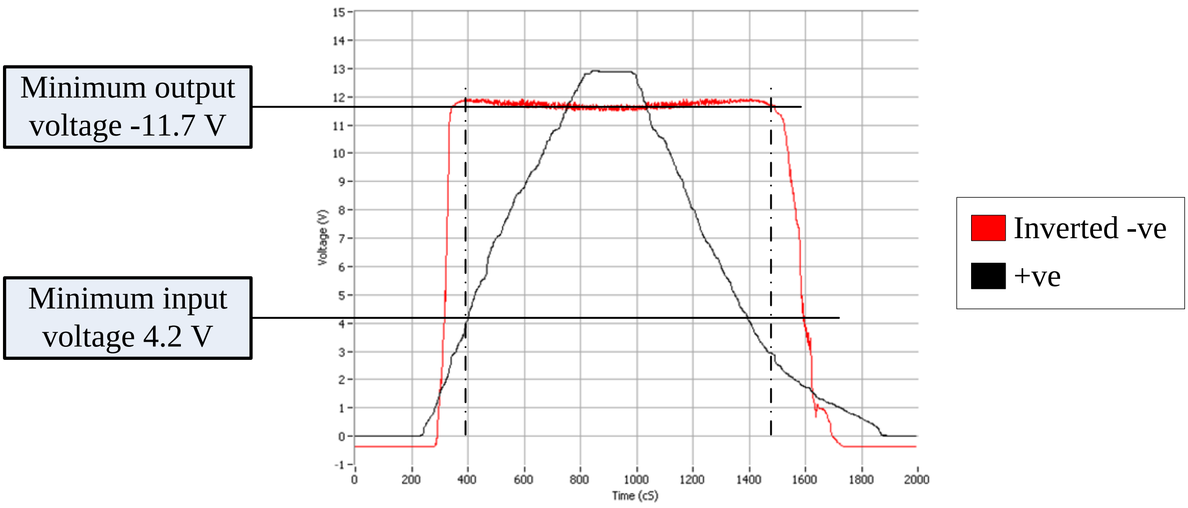


**Figure 5.21:** Dual power supply test showing minimum voltage supply needed

The second test was to observe the large oscillations in more detail. The output voltage was displayed on a separate graph in order to produce a higher resolution plot of the oscillations. It was observed that as the input voltage was increased, the output voltage oscillation difference increased as well (Figure 5.22). Therefore, the original input of 12 V was reconsidered and the output reduced to approximately 7.5–9 V. This lowered voltage was still suitable for the amplifiers as they required a minimum of 5 V.

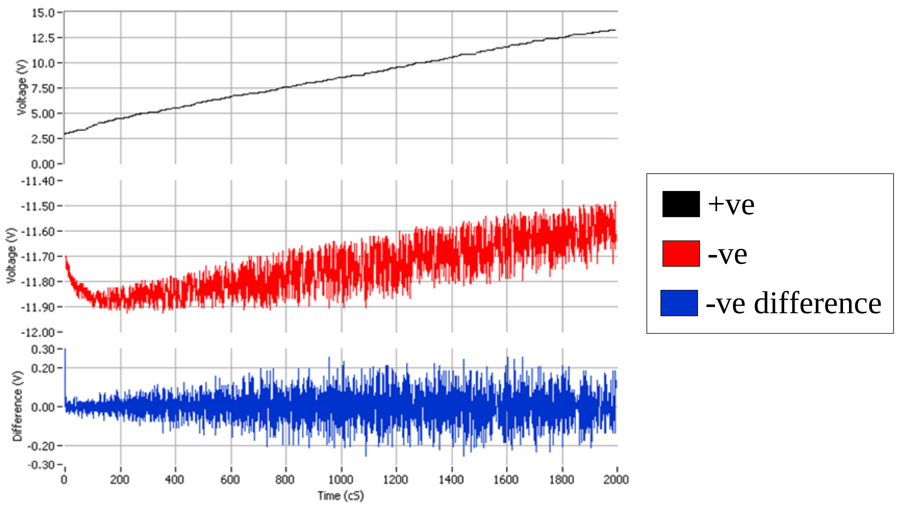


**Figure 5.22:** Higher resolution showing increased noise as the voltage supply is increased

## 5.4 High frequency testing

As the DAQ hardware did not have the capability to observe the constructed electrical sensors at a high sampling rate an oscilloscope was used. The DAQ hardware is only capable of a maximum sampling rate of 50 kHz with a resolution of 2.441 mV. However, the sampling rate was set at only 100 Hz in LabVIEW.

The dual polarity power supply was tested first as this was thought to be the source of the created noise due to its switch mode operation. The dual polarity power supply was tested without a load. It was observed that the power supply was in fact a saw wave on the negative output (Figure 5.23). The wave had a frequency of 394.3 Hz and a peak-to-peak voltage of approximately 330 mV.

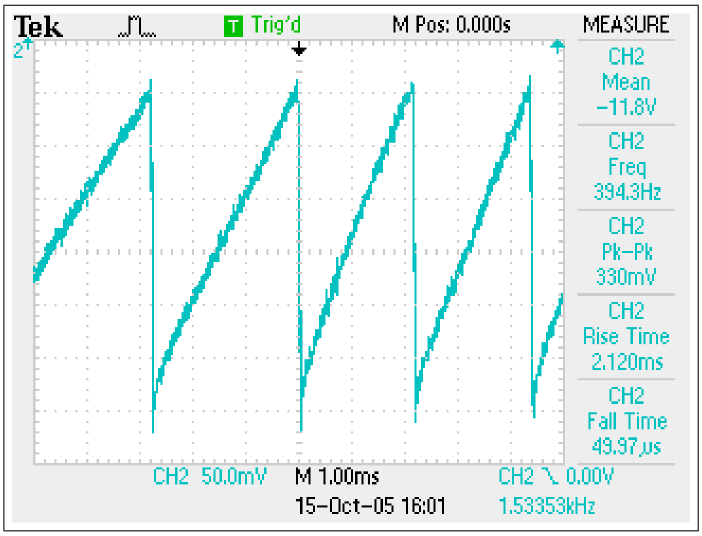


**Figure 5.23:** Dual power supply test, negative output with no load

However, testing the circuit without a load was not a good representation of the performance of the circuit. Hence, the dual polarity power supply was connected to the voltage sensor (Figure 5.24). Operating with a load, placed the sensor under similar conditions as when connected to the DAQ hardware.

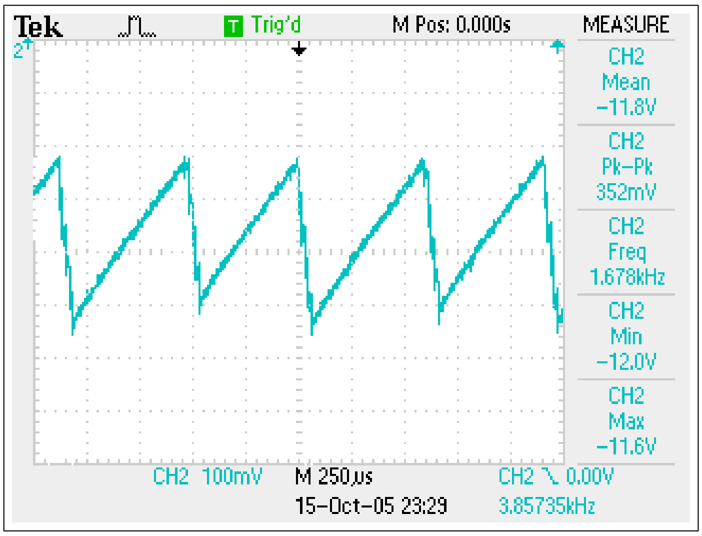


**Figure 5.24:** Dual power supply test, negative output with load

Again, a saw wave was observed, but on this occasion it was at a frequency of 1.678 kHz. The peak-to-peak voltage was approximately the same as the previous tests, at 352 mV.

Testing the voltage sensor was mainly to observe if there was any noise that the DAQ hardware was filtering (Figure 5.25). It was observed that there were large spikes in the voltage out that were not being detected by the DAQ hardware. The frequency of these spikes were 60.95 kHz .

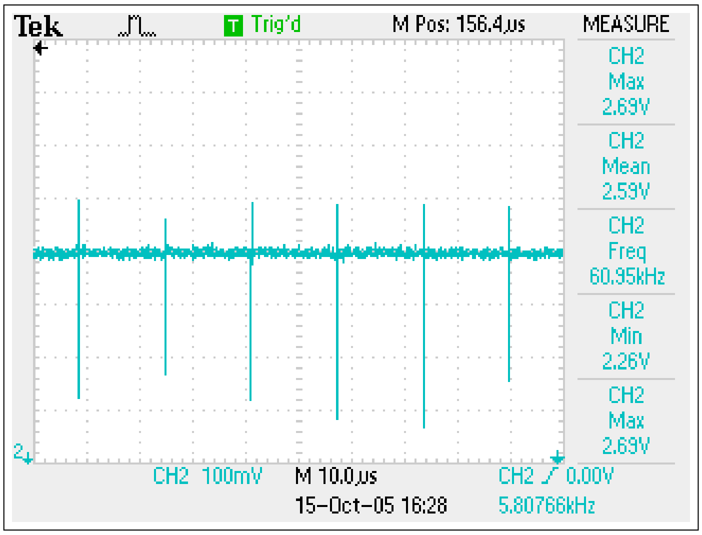


**Figure 5.25:** Voltage sensor test with oscilloscope

Finally, the current sensor was tested with the 50 mm and 200 mm shunt to determine the source of the original noise (Figure 5.26). Similar to the voltage sensor test, large spikes were observed. A minimum and maximum of -0.96 V and 8.64 V respectively was calculated with the oscilloscope, and hence these spikes may have been the cause of the original oscillations detected by the DAQ hardware.

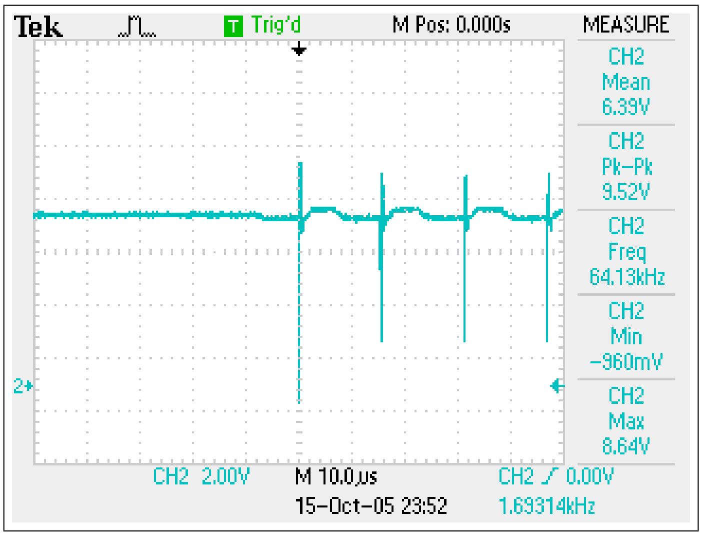


**Figure 5.26:** Current sensor test with 200 mm shunt, spikes can be observed

On closer observation it was observed that these spikes were smooth waves approximately 1 $\mu$s in length (Figure 5.27).

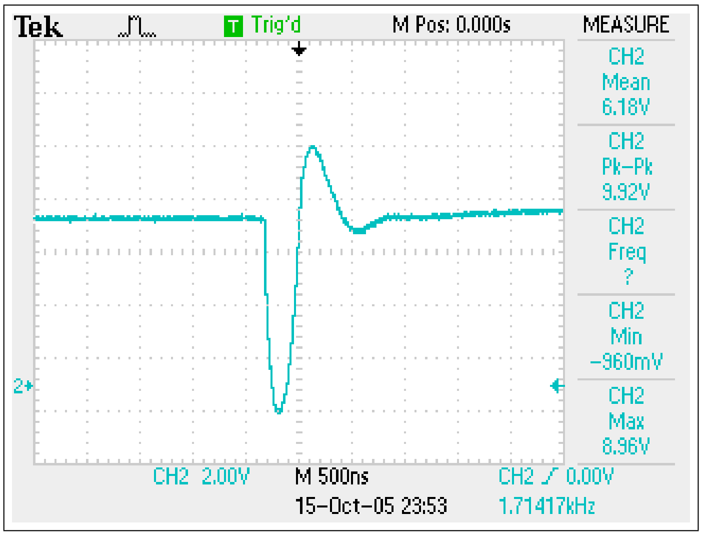


**Figure 5.27:** Current sensor test with 200 mm shunt, zoomed in on a single spike

Methods for removing these voltage spikes have been discussed in Chapter 7 in the section on future work.

# Chapter 6

# Temperature

There are numerous temperature measurements required for various parts of the vehicle. These include air temperatures in the driver's compartment and on components that have a specific operating temperature, such as motors, electrical components and the fuel cell.

## 6.1 Low temperatures

Low temperature measurements (generally between 0 °C to 100 °C) were the most simple to implement using integrated-circuit temperature sensors and these could be purchased easily and inexpensively. Analog Devices [33] make the TMP35 [38] a low voltage, precision centigrade temperature sensors with a range of 10–125 °C. It provides a voltage output that is linearly proportional to the Celsius temperature.

The sensor's power supply maximum was 5.5 V, so a 5 V regulator was used to allow a larger power voltage range.

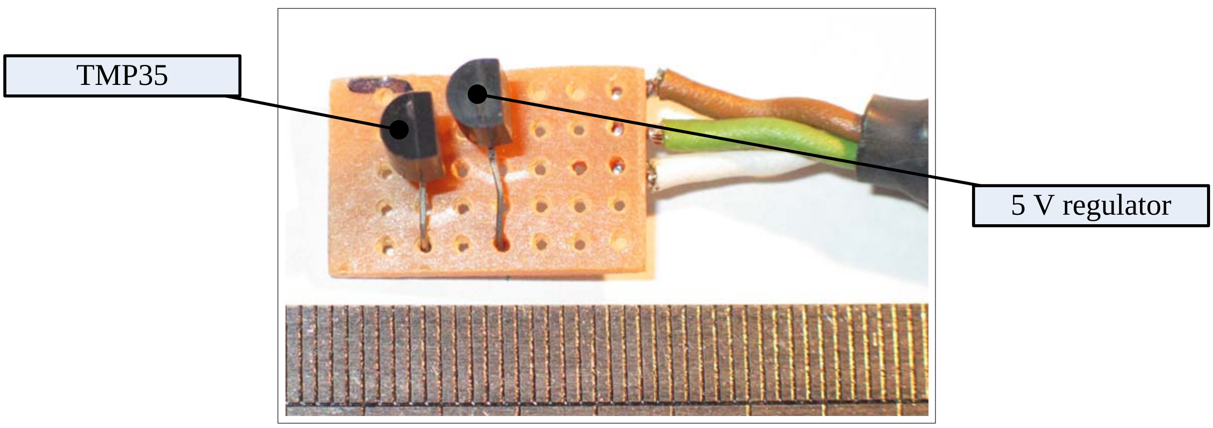


**Figure 6.1:** TMP35 temperature sensor with 5 V regulator on a PCB

### 6.1.1 Calibration

The initial testing was to confirm the sensor was calibrated correctly. The sensor and a household alcohol thermometer were placed close to each other and left to settle at room temperature for one hour. Thereafter, the two readings were taken. The household thermometer read 17 °C with ±1 °C accuracy as specified by the manufacturer, and the temperature sensor read 173 mV with an accuracy of ±19.766 mV (as specified by the DAQ hardware manufacturer located in Appendix D). The temperature sensor used a scale factor of 10 mV/°C. The sensor reading then equated to 17.3±1.9766 °C, which was the same as the household thermometer's reading of 17±1 °C, with a maximum relative error of ±1.639 °C.

One factor that was not considered when populating the components onto the PCB was robustness. The three pin plastic header style packaging (TO-92) was very susceptible to breaking and on a number of occasions the chips' legs were either squashed or the chips ripped off completely. To prevent this, the chips were glued onto the PCB flat side down (Figure 6.2).

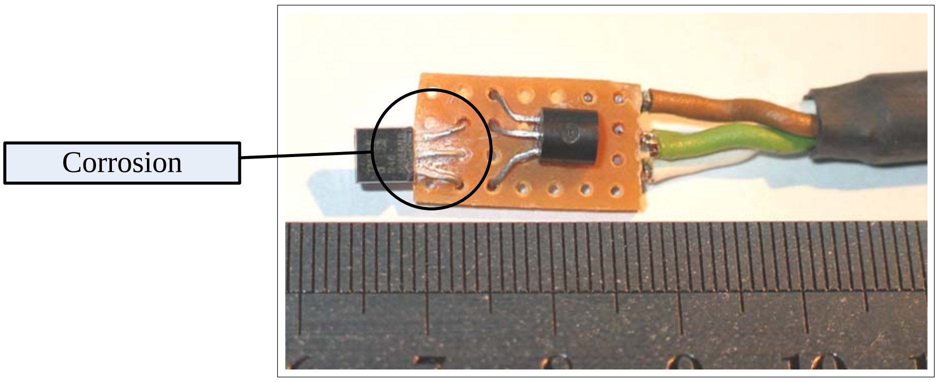


**Figure 6.2:** Modified temperature sensor, corrosion can be seen due to being submerged in water

Since the temperature sensor had a minimum of 10 °C, it was not possible to perform tests using icy water. Instead, a warm solution of demineralised water was used for the second test, as at that time it was thought to be an insulator. During the test when the sensor was submerged, it was evident that the demineralised water was still conducting electricity and had altered the output voltage signal.

A new temperature sensor was used that was soldered directly onto 3-cored cable with heat shrink used as insulation. To seal the sensor from water, clear lacquer was applied to any exposed wire (Figure 6.3). The sensor was again submerged in water and the voltage out reading did not change, hence confirming that it was insulated.

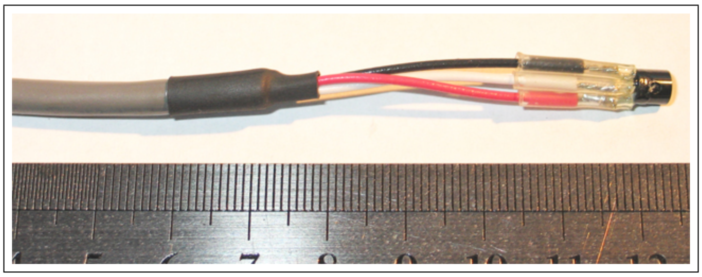

**Figure 6.3:** TMP35 temperature sensor directly connected to 3-core cable

When both the temperature sensor and household thermometer were submersed in warm water, the temperature sensor outputted 429.7 mV with an accuracy of ±19.766 mV, which equated to 42.97±1.9766 °C. This was again the same as the household thermometer that read 43.5±1 °C. There was a maximum relative error of ±1.753 °C.

### 6.1.2 Testing

A number of tests were conducted on the temperature sensors to observe their characteristics. The first test was to observe their response time. A cup of mineral oil with one temperature sensor was heated up to 97.2±1.9766 °C. The second temperature sensor was then placed into the oil and its response time was observed to be 37±1 s (Figure 6.4). Hence, the temperature sensor would not be useful in situations of quick temperature changes. This, however, would not be a problem as most temperatures in the REV change gradually.

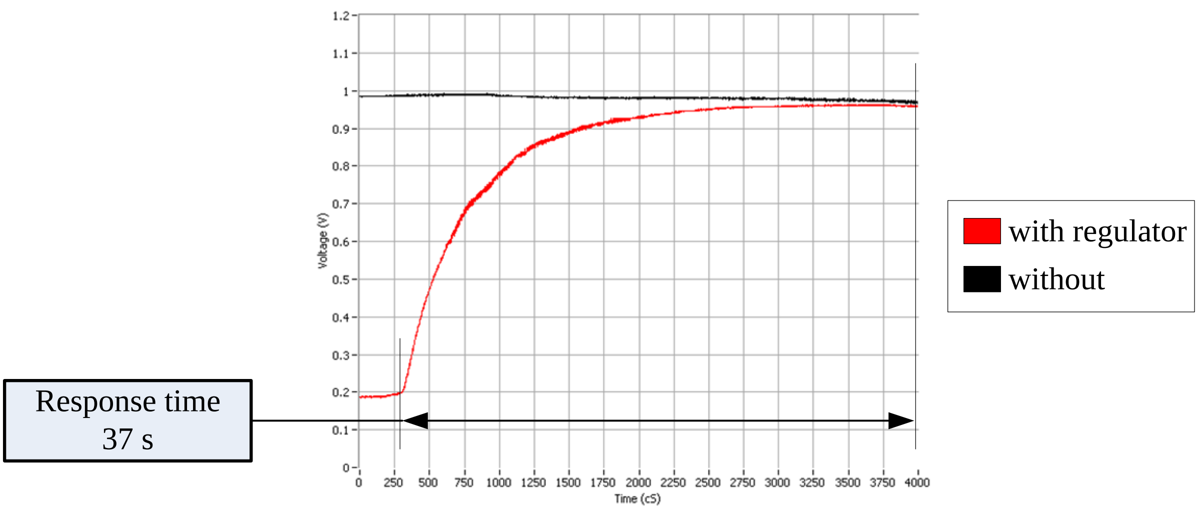


**Figure 6.4:** Response of the temperature sensors when submerged in hot oil

The second test was to observe the sensor's minimum detection temperature. The sensor was placed in icy water (approximately 0 °C) and the minimum measured temperature recorded (Figure 6.5). It was observed that a minimum of 0.6 V was obtained which corresponded to 6 °C. The minimum detection temperature is stated as 10 °C. This was confirmed when the water was at 0 °C and an incorrect reading of 6 °C was obtained. This minimum reading did give a good indication of what the sensor would output at temperatures lower than specified and this could be used as an error voltage when the sensor is operating outside its specified minimum temperature.

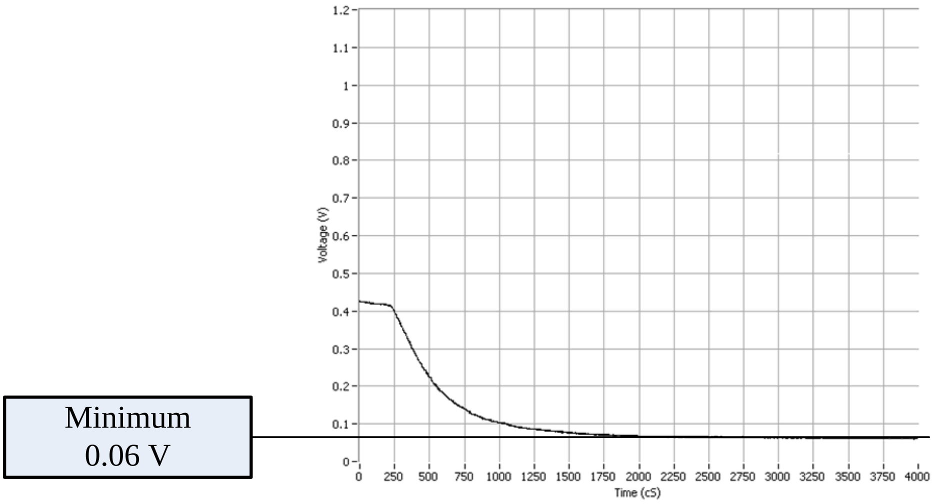


**Figure 6.5:** Response of the temperature sensor when submerged in icy water

The final test was to observe how the two temperature sensors responded to a varying power supply, and at what voltages did the temperature sensors output correctly. The temperature sensors' power supply was gradually increased from 0 V to approximately 15 V and the voltage output recorded.

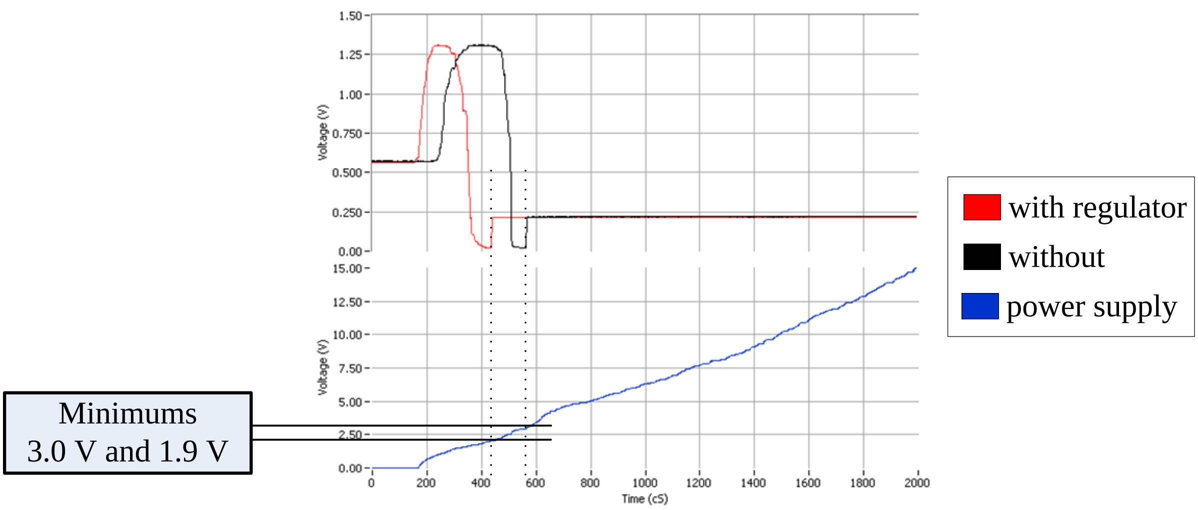


**Figure 6.6:** Response of the temperature sensors with a varying power supply

It was observed that the temperature sensors gave correct outputs when the power supply was at least 3 V. At voltages lower than this, 'false' readings occurred. Thus, if there were power supply problems, the sensors could give higher readings than the actual temperature and may cause components to shut down due to assuming that they are overheating. However, multiple temperature sensors could be used to prevent these errors.

## 6.2 Temperature effect on electrical components

Many components are susceptible to temperature and their characteristics change as the temperature changes. Tests were conducted on the most common component; resistors, to observe to what extent temperature affected them.

### 6.2.1 Resistors

The resistance of resistors change as temperature changes. Through the following test, the actual resistance change was calculated and used to determine if this would change sensor readings enough to cause a problem. The test involved testing three different types of resistors; carbon film, wire wound, and metal film all with approximately the same resistance (Figure 6.7). The resistors were submerged into white oil (a non-conductive oil verified with an insulation tester) and the resistance recorded at various temperatures using a multimeter (Table 6.1).

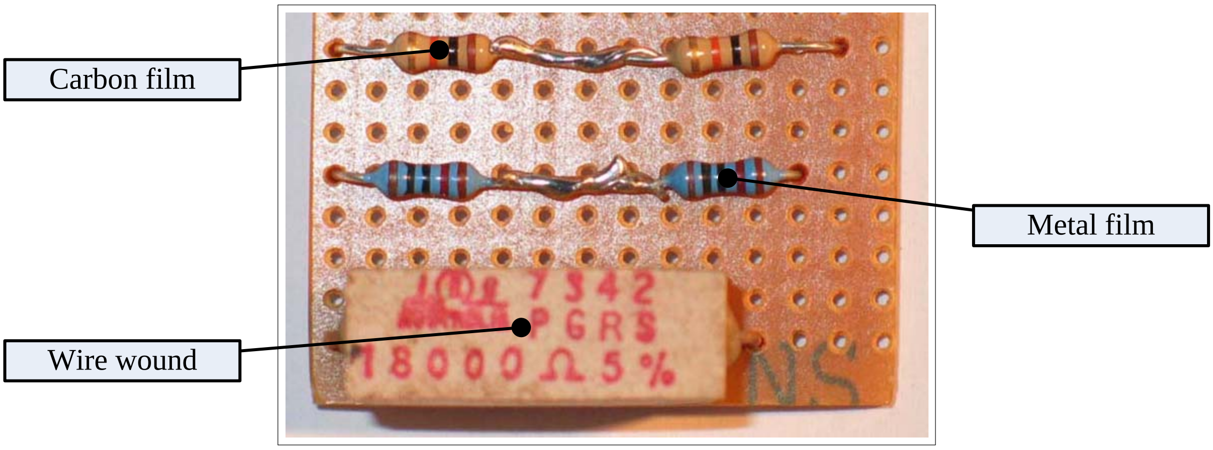


**Figure 6.7:** Three resistor types used for testing

Due to the resistors having slightly different resistances, the percentage change was calculated. The room temperature (20.51 °C) readings were used as the reference resistance (Table 6.2). The percentage change per degree Celsius was then plotted (Figure 6.8).

Table 6.1: Temperature change at various temperatures

| Temperature (°C) | Resistance (kΩ) | | |
|---|---|---|---|
| | Carbon film | Metal film | Wire wound |
| -18±1 | 20.05±0.028045 | 20.05±0.028045 | 18.37±0.026533 |
| 20.51±1.9766 | 19.84±0.027856 | 20.03±0.028027 | 18.39±0.026551 |
| 54.93±1.9766 | 19.69±0.027721 | 20.01±0.028009 | 18.40±0.02656 |
| 82.03±1.9766 | 19.53±0.027577 | 20.00±0.028 | 18.40±0.02656 |

Table 6.2: Percentage change at various temperatures

| Temperature (°C) | Change (%) | | |
|---|---|---|---|
| | Carbon film | Metal film | Wire wound |
| -18±1 | 1.06 | 0.10 | -0.11 |
| 20.51±1.9766 | 0.00 | 0.00 | 0.00 |
| 54.93±1.9766 | -0.76 | -0.10 | 0.05 |
| 82.03±1.9766 | -1.56 | -0.15 | 0.05 |

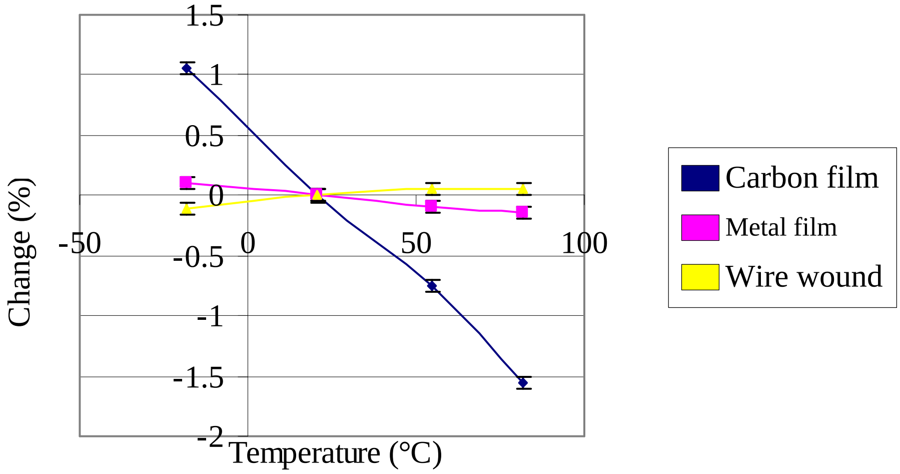


**Figure 6.8:** Percentage change per temperature of the three resistor types

Initial observations showed that carbon film resistors varied significantly, whilst metal film and wire wound varied slightly. One distinct noticeability was that the wire wound resistor's resistance increased with temperature, whilst the carbon and metal film decreased. The change in resistance with temperature was linear, and hence a trendline was created (Figure 6.9). The equation of the trendline was important, specifically the gradient, which was the percentage change per degree Celsius or temperature coefficient (TC).

The temperature coefficients can be used to approximate the temperature change of resistors with a similar resistance to that of the test resistors, but the TC cannot be used

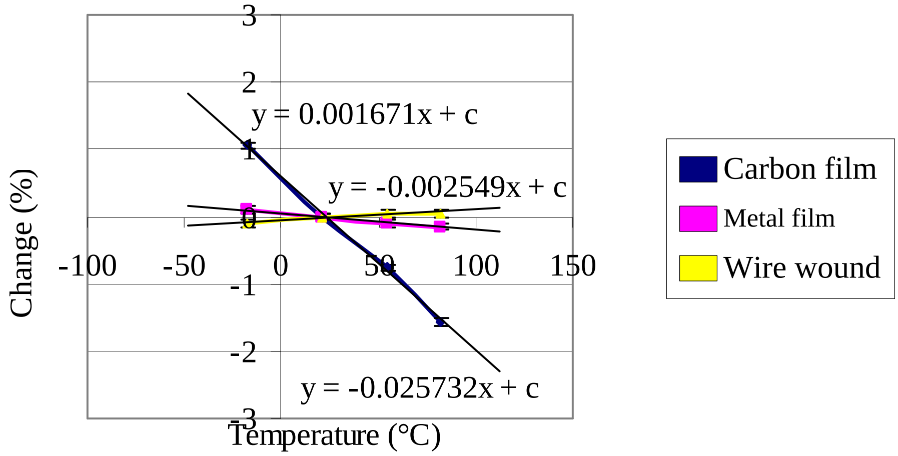


**Figure 6.9:** Percentage change per temperature of the three resistor types with linear trendline added

**Table 6.3:** Temperature coefficient of the various resistor types

| **Resistor type** | **Calculated TC** (%/°C) | $R^2$ value |
|---|---|---|
| Carbon film | −0.025732 | 0.997339 |
| Metal film | −0.002549 | 0.994661 |
| Wire wound | 0.001671 | 0.885916 |

for different resistances as this changes. The relationship between TC and resistor values are not linear, and hence will need to be determined by looking at manufacturers' data sheets. An example TC plot for carbon film resistors is seen in Figure 6.10. Hence, using the example TC curve for a 0.25 W carbon film resistor, a 20 kΩ resistor had a TC of $-0.033 \pm 0.001$ %/°C when compared with the calculated value of $-0.025732$ %/°C it was quite close. The differences were due to the actual resistors used not being produced by the same manufacture that produced the plot. However, it did give a good indication of the expected TC of carbon film resistors.

Taking into account the temperature change, this data can then be used to determine the effect of temperature on the voltage and current sensors. In both cases a carbon film resistor was used as an example as they had the highest TC. However, in the actual design metal film or wire wound would be used. For both sensors an extreme case was considered, a temperature change of 100 °C.

#### 6.2.1.1 Voltage sensor

Resistors were used as the main component of the voltage sensor in the voltage divider circuit. Assuming that the sensor was perfectly constructed with a $V_{in}$:$V_{out}$ ratio of 1:3

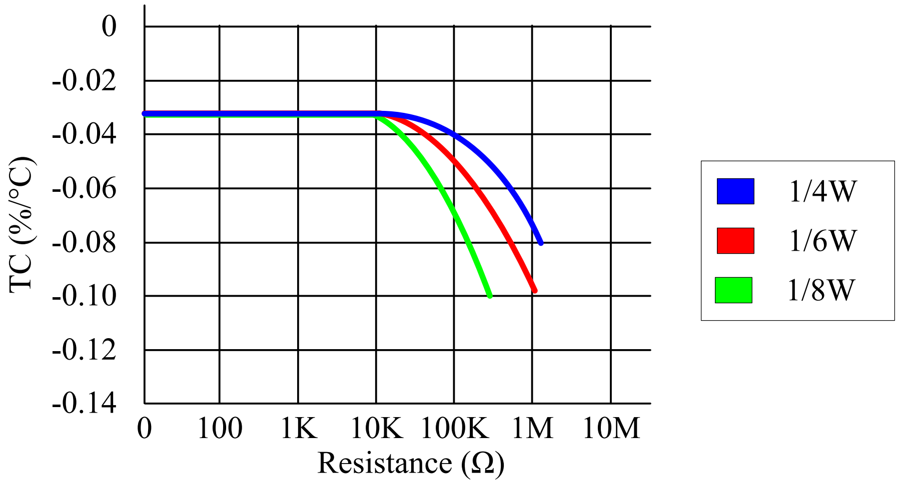


**Figure 6.10:** Example TC plot for carbon film resistors [2]

and hence designed with 392 kΩ and 196 kΩ resistors, having a TC of −0.057 %/°C and −0.046 %/°C respectively. A temperature change of 100 °C resulted in modified resistor values of 369.656 kΩ and 186.984 kΩ respectively. This resulted in a new temperature ratio of 1.0077:3. Therefore, it affected the voltage divider by approximately 0.77 %. Even with extreme temperature, the change was insignificant.

#### 6.2.1.2 Current sensor

The main concern with the current sensor was the use of the resistor to program the instrumentation amplifier's gain. A 47.35 Ω resistor was used to produce a gain of approximately 1044. Hence, the resistor had a TC of −0.0315 %/°C and with a temperature change of 100 °C resulted in a resistor value of 45.86 Ω. This resulted in a gain of 1078, which was an increase by 3.26 %.

## 6.3 Methods to minimise the effect of temperature

Methods to prevent incorrect values occurring due to temperature changes, include using the following:

**Temperature sensors** — These are located around the sensor and updating the sensor readings in software using a temperature look-up table.

**Components that have a low TC** — These include wire wound resistors but are considerably more expensive.

**Temperature compensating circuits** — These use two similar components that cancel any change due to temperature.

**Cooling fans** — These prevent any large change in temperatures occurring.

# Chapter 7

# Conclusions and further work

Initially the general sensor selection criteria and conditions which included performance specifications, operating specifications and costs were discussed. As it is extremely difficult to find a suitable sensor that matches all criteria, sensor testing is imperative.

General sensor testing methods were also discussed and these included checking sensor calibration, testing the sensor under extreme conditions and finally the methods available to maximise the sensor's performance. These included placing the sensor in a specific position to maximise its operation or simply protecting the sensor in an enclosure.

## 7.1 Measurements discussed

Three different required measuring quantities were looked at and these included hydrogen concentration, electrical and temperature. These accounted for over 70 % of the required measurements in the REV.

### 7.1.1 Hydrogen concentration

The hydrogen concentration sensor was required due to safety reasons. Hydrogen would be needed for testing and running the fuel cell. Hence, it was critical that any hydrogen leaks were detected.

Three sensors where purchased from the company Neodym Technologies [1] that met the sensor selection criteria; two MiniKnowzs for the final REV and one Panterra-CAT for use in the hydrogen testing workshop.

The first tests that were performed on the sensors were calibration checking. A known concentration of hydrogen and air was created and the sensors submerged into it. It was found that the sensors did output as expected. The second test was initially to observe if car exhaust caused ‘false’ readings with the sensors, which it did. In order to determine if the sensors were still useable the sensors were placed inside a car to simulate the REV, there were no significant readings.

The sensors are suitable for use in the REV. From the tests that were conducted, the author is confident that the sensors would work as anticipated when finally placed in the REV.

### 7.1.2 Electrical

Rather than being purchased the electrical sensors were designed and constructed specifically for the REV.

The voltage sensors were designed based on a simple voltage divider circuit and a voltage follower circuit. A design suitable for a maximum voltage of 15 V was constructed and tested. It was observed that it did scale the voltage as expected. The sensor would be suitable for use in the REV.

The current sensors were based on a shunt resistor measuring the voltage across it with an instrumentation amplifier. The current sensors showed that they did produce a voltage signal that was linearly proportional to the current.

### 7.1.3 Temperature

Simple integrated-circuit temperature sensor were suitable for low temperature measurements. The TMP35 [38] was confirmed to be calibrated correctly and the response times observed in high and low operating temperatures. The temperature sensors were verified to work between the temperature range of approximately 6 °C to 95 °C. Methods of insulating the sensors from conductive liquids were also discussed. Due to the sensors being low-priced they are a very simple and effective device for measuring temperatures around the REV.

The temperature effect on resistors was also tested. Three different types of resistors were tested and their temperature coefficient calculated. It was found that the experimental values did agree with the data from manufactures. Finally, it was calculated to what extent a temperature change of 100 °C would affect the current and voltage sensors if they were designed with carbon film resistors. The voltage sensor input/output ratio was affected by 0.77 % and the current sensors gain was affected by 3.26 %. Even at extreme cases, the effect was quite small. Different methods were finally discussed to minimise sensors' susceptibility to temperature changes.

## 7.2 Further work

The sensor tests discussed in this thesis have produced useful information on the sensors' performance. However, there are a number of tests that can be conducted to determine further sensor specifications.

### 7.2.1 Hydrogen concentration

It may be useful to determine the response time of the sensors subjected to higher concentrations of hydrogen gas. When large leaks occur an extremely fast response time is needed. However, testing with larger concentrations of hydrogen creates a hazardous environment.

Similar to the tests conducted with car exhaust, other gases can be used to determine if they too caused 'false' readings. Individually testing the components that constitutes car exhaust would single out the specific gases that caused 'false' readings.

As the REV further develops in design and construction, the precise location of the sensors and their fixtures could be determined which would also include the method to remove the sensor for servicing.

### 7.2.2 Electrical

Due to the REV having a large number of voltage measurements, it may be simpler to create etched PCBs that consisted of a dual polarity power supply combined with the voltage sensor. This would minimise any noise being detected on the wires that would normally connect each other. Multiple op-amps are usually combined onto the single chip, hence a voltage sensor design could be incorporated where multiple voltage measurements can be acquired from the single voltage sensor, saving space and weight.

The current sensor's principle worked as expected. One problem was noise being detected in the voltage signal. This noise can be minimised by using a specifically designed shunt resistor that does not vary with temperature and is designed to minimise the amount of detected noise. Further tests should then be conducted to observe if the noise is still occurring.

There are a number of filtering methods that can be added to the current sensor circuit to remove the voltage spikes. However, the simplest method is by adding a passive filter made with capacitors, inductors or resistors. A low-pass filter would be needed to remove the high frequency spikes.

### 7.2.3 Temperature

The temperature sensors' calibration was tested relative to an alcohol thermometer and then relative to each other. Ideally, a pre-calibrated thermometer should have been used when checking the sensors' calibration. This pre-calibrated thermometer should have a sensing range below 0 °C to above 150 °C. Due to safety reasons the temperature sensors were not checked above 100 °C as oil at this temperature was hazardous. However, this could be undertaken in a laboratory environment with the correct apparatus.

The influence of temperature on resistors was discussed. The effect of temperature change on other components, such as integrated-circuits should also be tested.

### 7.2.4 General sensor selection

There is still a great deal of work to be done on sensor selection and testing for the REV. The selection process of the remainder of required sensors (approximately 30 %) is almost finalised, but testing methods still need to be developed and completed. Hopefully, with the information that has been outlined in this thesis, the job of sensor selection and testing will be made easier for the REV and any future projects that require sensors.

# References

[1] (2005) Neodym Technologies Inc. Vancouver, Canada. [Online]. Available: http://www.neodymsystems.com

[2] W. C. Limited. (2002) General purpose carbon film resistors. GCF.PDF. http://www.welwyn-tt.com/pdf/datasheet/GCF.PDF.

[3] R. H. Bishop, *The Mechatronics Handbook.* CRC Press, 2002.

[4] A. B. of Statistics. (2003) Geography and climate temperature. [Online]. Available: http://www.abs.gov.au/Ausstats/abs@.nsf/0/b5186097bad6b76cca256b3400819cd1

[5] (2005) GlobalSpec Inc. Troy, New York. [Online]. Available: http://www.globalspec.com

[6] (2005) Laboratory for Measurement & Instrumentation. University of Twente, The Netherlands. [Online]. Available: http://www-mi.el.utwente.nl

[7] (2003) KISIS, Knowledge based Intelligent system for the Selection of Industrial Sensors. University of Twente, The Netherlands. [Online]. Available: http://www.mi.el.utwente.nl/ksn/research/kisis/

[8] M. Korsten, P. van der Vet, and P. Regtien, "A system for the automatic selection of sensors," in *Proc. IMEKO (International Measurement Confederation) XVI*, Vienna, Austria, Sept. 2000, pp. 211–216. [Online]. Available: http://www.mi.el.utwente.nl/ksn/research/kisis/Publications.htm

[9] P. P. Regtien, "Selection of sensors," in *Handbook of Measuring System Design.* John Wiley & Sons, Ltd, 2005, ch. 116. [Online]. Available: http://eu.wiley.com/legacy/wileychi/hbmsd/pdfs/mm069.pdf

[10] W. B. Ribbens, *Understanding Automotive Electronics.* Newnes, 1998.

[11] A. W. M. Bonnick, *Automotive Computer Controlled Systems.* Butterworth-Heinemann, 2001.

[12] R. Bosch, "Automotive Sensors Basics," in *Bosch Automotive Sensors.* Bentley Publishers, 2005. [Online]. Available: http://www.boschautoparts.co.uk/pdf/3-934584-50-0.pdf

[13] M. Nadal and F. Barbir, "Development of a hybrid fuel cell/battery powered electric vehicle," *International Journal of Hydrogen Energy*, vol. 21, pp. 497 – 505, 1996.

[14] L. Cardinali, S. Santomassimo, and M. Stefanoni, "Design and realization of a 300 W fuel cell generator on an electric bicycle," *Journal of Power Sources*, vol. 106, pp. 384 – 7, 2002.

[15] J. G. Webster, *The Measurement, Instrumentation and Sensors Handbook.* CRC Press, 1999.

[16] W. Boyes, Ed., *Instrumentation Reference Book.* Butterworth-Heinemann, 2003.

[17] Safety Standard for Hydrogen and Hydrogen Systems. Washington DC. [Online]. Available: http://www.hq.nasa.gov/office/codeq/doctree/871916.pdf

[18] A. P. Jardine. (2000) Hydrogen Sensors for Hydrogen Fuel Cell Applications. [Online]. Available: http://www.powerpulse.net/powerpulse/archive/aa_111300a1.stm

[19] P. Riiedi, P. Heim, A. Mortua, E. Franzi, H. Oguey, and X. Arreguit, "Interface Circuit for Metal-Oxide Gas Sensor," in *Custom Iintegrated Circuits Conference.* Neuchatel, Switzerland: IEEE, 2001.

[20] A. D. Brailsford, M. Yussouff, and E. M. Logothetis, "Theory Of Metal Oxide Gas Sensors For Measuring Combustibles," in *International Conference on Solid-Safe Sensors and Actuators.* Dearbom, Michigan: IEEE, 1997.

[21] L. Makadmini and M. Horn, "Self-calibrating Electrochemical Gassensor," in *International Conference on Solid-Safe Sensors and Actuators.* Neubiberg, Germany: IEEE, 1997.

[22] J.F. Vetelino and J.C. Andle and R.S. Falconer, "Theory, design and operation of surface generated acoustic wave sensors," Maine, America, 1994.

[23] B. Drafts. (2000, Oct.) Acoustic Wave Technology Sensors. [Online]. Available: http://www.sensorsmag.com/articles/1000/68/main.shtml

[24] V.I.Anisimkin, "Russia-Italy Researches on Surface Acoustic Wave Gas Sensors," Moscow, Russia, 1996.

[25] W. Jakubik and M. Urbańczyk, "Hydrogen detection in Surface Acoustic Wave gas sensor based on interaction speed," Gliwice, Poland, 2004.

[26] "MiniKnowz Datasheet," MiniKnowz_Datasheet_100.pdf, 2005. [Online]. Available: http://www.neodymsystems.com/download/MiniKnowz_Datasheet_100.pdf

[27] B. McDonald, private communication, Neodym Technologies Inc., 2005.

[28] "Panterra-TCOND Product Brief," Panterra-TCOND_Brief_100.pdf, 2005. [Online]. Available: http://www.neodymsystems.com/download/Panterra-TCOND_Brief_100.pdf

[29] C. R. Nave. (2005) HyperPhysics. [Online]. Available: http://hyperphysics.phy-astr.gsu.edu/hbase/hph.html

[30] National Instruments. Austin, Texas. [Online]. Available: http://www.ni.com

[31] S. Acosta. (2005) Using a Unity Gain Buffer (Voltage Follower) with a DAQ Device. [Online]. Available: http://zone.ni.com/devzone/conceptd.nsf/webmain/CD57A73721E0612586256BAE0055CDD9

[32] (2005) STMicroelectronics. [Online]. Available: http://www.st.com

[33] Analog Devices, Inc. Norwood, Massachusetts. [Online]. Available: http://www.analog.com

[34] "AD620 - Low Drift, Low Power Instrumentation Amp with Set Gains of 1 to 10000," 2004. [Online]. Available: http://www.analog.com/en/prod/0%2C2877%2CAD620%2C00.html

[35] (2004) Calculation of electrical resistivity with copper. [Online]. Available: http://www.allmeasures.com/Formulae/static/formulae/electrical_resistivity/12.htm

[36] Maxim Integrated Products, Inc. Sunnyvale, California. [Online]. Available: http://www.maxim-ic.com

[37] "Preset/Adjustable Output CMOS Inverting Switching Regulators," 1999. [Online]. Available: http://www.maxim-ic.com/quick_view2.cfm/qv_pk/1381

[38] TMP35 - Voltage Output Temperature Sensors. Norwood, Massachusetts. [Online]. Available: http://www.analog.com/en/prod/0,,766_811_TMP35,00.html

[39] (2005) BOC Limited. Australia. [Online]. Available: http://www.boc.com.au

[40] (2004) Measurement computing corporation. http://www.measurementcomputing.com.

# Appendix A

# Required measurements on the REV

| Measurement | Code | Covered |
|---|---|---|
| **FUEL CELL** | | |
| Hydrogen pressure cylinder | H_PRESS_CY | |
| Hydrogen pressure in | H_PRESS_IN | |
| Hydrogen flow rate | H_FLOW | |
| Air pressure | A_PRESS | |
| Air flow rate | A_FLOW | |
| Air humidity 1 | A_HUMD_1 | |
| Air humidity 2 | A_HUMD_2 | |
| Air temperature | A_TEMP | ✓ |
| Water temperature in | W_TEMP_IN | ✓ |
| Water temperature out | W_TEMP_OUT | ✓ |
| Water flow rate | W_FLOW | |
| Oxygen concentration in | O_CONC | |
| Stack temperature 1 | ST_TEMP_1 | ✓ |
| Stack temperature 2 | ST_TEMP_2 | ✓ |
| Stack temperature 3 | ST_TEMP_3 | ✓ |
| Stack temperature 4 | ST_TEMP_4 | ✓ |
| Stack temperature 5 | ST_TEMP_5 | ✓ |
| Stack temperatures rolling[1] (5) | ST_TEMP_R | ✓ |
| Fuel cell voltages rolling (5) | CELL_V_R | ✓ |

[1]Rolling — measurements that are not required to be continuously sampled and hence can be multiplexed together

| | | |
|---|---|---|
| Stack current | ST_I | ✓ |
| Stack voltage | ST_V | ✓ |
| Hydrogen leak sensor 1 | H_LEAK_1 | ✓ |
| Hydrogen leak sensor 2 | H_LEAK_2 | ✓ |
| Hydrogen leak sensor 3 | H_LEAK_2 | ✓ |
| **ELECTRICAL** | | |
| Capacitor voltage | CAP_V | ✓ |
| Capacitor current | CAP_I | ✓ |
| Capacitor current bus | CAP_I_BUS | ✓ |
| Voltage bus | V_BUS | ✓ |
| Solar voltage 1 | SOL_V_1 | ✓ |
| Solar voltage 2 | SOL_V_2 | ✓ |
| Solar voltage 3 | SOL_V_3 | ✓ |
| Solar voltage 4 | SOL_V_4 | ✓ |
| Solar voltage 5 | SOL_V_5 | ✓ |
| Solar current 1 | SOL_I_1 | ✓ |
| Solar current 2 | SOL_I_2 | ✓ |
| Solar current 3 | SOL_I_3 | ✓ |
| Solar current 4 | SOL_I_4 | ✓ |
| Solar current 5 | SOL_I_5 | ✓ |
| Net solar current | SOL_I_NET | ✓ |
| Solar current bus | SOL_I_BUS | ✓ |
| Fuel cell current bus | FC_I_BUS | ✓ |
| Right motor current | MOTR_I | ✓ |
| Right motor phase current A | MOTR_I_A | ✓ |
| Right motor phase current B | MOTR_I_B | ✓ |
| Right motor phase current C | MOTR_I_C | ✓ |
| Right hall effect 1 | MOTR_H_1 | |
| Right hall effect 2 | MOTR_H_2 | |
| Right hall effect 3 | MOTR_H_3 | |
| Left motor current | MOTL_I | ✓ |
| Left motor phase current A | MOTL_I_A | ✓ |
| Left motor phase current B | MOTL_I_B | ✓ |

| | | |
|---|---|---|
| Left motor phase current C | MOTL_I_C | ✓ |
| Left hall effect 1 | MOTL_H_1 | |
| Left hall effect 2 | MOTL_H_2 | |
| Left hall effect 3 | MOTL_H_3 | |
| 12V bad voltage | 12VB_V | ✓ |
| 12V bad current bus | 12VB_I_BUS | ✓ |
| 12V bad current | 12VB_I | ✓ |
| 12V stable current bus | 12VS_I_BUS | ✓ |
| Start up battery voltage | START_V | ✓ |
| Start up battery current | START_I | ✓ |
| Battery cell voltage rolling (5) | BATT_V_R | ✓ |
| Battery current | BATT_I | ✓ |
| Electrical temperature 1 | E_TEMP_1 | ✓ |
| Electrical temperature 2 | E_TEMP_2 | ✓ |
| Electrical temperature 3 | E_TEMP_3 | ✓ |
| Electrical temperature 4 | E_TEMP_4 | ✓ |
| Electrical temperature 5 | E_TEMP_5 | ✓ |
| Electrical temperature 6 | E_TEMP_6 | ✓ |
| Electrical temperature 7 | E_TEMP_7 | ✓ |
| Electrical temperature 8 | E_TEMP_8 | ✓ |
| Electrical temperature 9 | E_TEMP_9 | ✓ |
| Electrical temperature 10 | E_TEMP_10 | ✓ |
| Electrical temperatures rolling (5) | E_TEMP_R | ✓ |
| **DYNAMICS** | | |
| Angular rate roll | ANG_ROLL | |
| Angular rate pitch | ANG_PITCH | |
| Inclinometer roll | IN_ROLL | |
| Inclinometer pitch | IN_PTCH | |
| Ambient temperature | AB_TEMP | ✓ |
| Ambient humidity | AB_HUM | |
| Steering wheel angle | ST_ANG | |
| Brake pedal | BRAKE | |
| Accelerator pedal | ACCEL | |

| | |
|---|---|
| Right brake temperature | BR_TEMP_R |
| Left brake temperature | BR_TEMP_L |
| Left wheel velocity | VEL_L |
| Right wheel velocity | VEL_R |

There are approximately 104 required measurements, 76 of the measuring types have been covered in this thesis.

# Appendix B

# Hydrogen concentration sensor testing procedure

The use of hydrogen for the sensor calibration has been approved by the University's Safety & Health Office and a Safety Assessment conducted by the School of Mechanical Engineering Safety Officer, Rob Greenhalgh (Appendix F).

The testing of sensors requires a known concentration of hydrogen and air mixture to be generated. This is done in two steps, the first is obtaining a small quantity of hydrogen gas directly from the cylinder and storing this in a balloon. The second part involves producing the hydrogen and air mixture.

## B.1 Obtaining a quantity of hydrogen

The School of Mechanical Engineering purchases all gases from BOC Australia [39]. BOC produces three hydrogen types (Table B.1), that are available in two cylinder sizes. Size D, the smallest available cylinder holds $1.2\,\mathrm{m}^3$ at STP and size E holds $3\,\mathrm{m}^3$ at STP.

Ideally the Ultra High Purity would be most suitable as this would create the most accurate gas mixture, unfortunately due to cost restrictions the Industrial Grade was used and may have to be used for future testing.

**Table B.1:** Available hydrogen grades from BOC

| Name | Minimum Purity | Price | |
|---|---|---|---|
| | | Size D | Size E |
| Industrial Grade | 99.5 % | $45.30 | $62.02 |
| High Purity | 99.98 % | $99.83 | $178.36 |
| Ultra High Purity | 99.999 % | $215.17 | $219.67 |

### B.1.1 Guidelines for safe hydrogen gas use

Before any hydrogen is used, the tester must

- Familiarise themselves with the MSDS for the chosen hydrogen grade, The MSDS can be located on BOC's website.
- Read the Safety Assessment (Appendix F) conducted by the School of Mechanical Engineering Safety Officer, Rob Greenhalgh.
- Read the following testing procedure thoroughly.
- Complete the Safety Checklist.

When using hydrogen gas, Personal Protective Equipment (PPE) must be worn. PPE includes:

- Eye protection (safety glasses can be obtained free from the mechanical office)
- Non-sparking clothing (cotton cloths that minimise static buildup)
- Closed toe, non-porous shoes (no thongs or sandals)

Whenever working with hydrogen, all potential ignition sources must be eliminated, sources of ignition include:

- Open flames (including personnel smoking)
- Electrical equipment
- Static electricity (nylon clothing)
- Heating equipment in buildings

### B.1.2 Preparing the cylinder

To order a cylinder of hydrogen, a mechanical workshop staff member must be informed and must also supervise the use of the cylinder.

Hydrogen cylinders are stored locked up outside the mechanical workshop. Hydrogen cylinders are always identified as being bright red in colour (Figure B.1). To use the cylinder it must be moved out of the cage, this increases ventilation and moves the experiment away from the other stored cylinders. A cylinder trolley designed for the specific cylinder size must be used when moving the cylinder. This makes the job of moving the cylinder easier, and also prevents the cylinder from tipping over which may break the regulator, and this is extremely dangerous.

Cylinders arrive without any attachments and hence a specific hydrogen regulator will need to be screwed onto the cylinder. A regulator restricts the outlet pressure and also provides a outlet to attach a balloon. Finally, a cylinder key is required to open the cylinder's valve (Figure B.2).


**Figure B.1:** Red hydrogen cylinder (size E) on cylinder trolley

### B.1.3 Filling the balloon

Before any hydrogen is released, the work area must be checked again to make sure there are no possible ignition sources. The balloon is placed over the regulator's outlet, the cylinder key can be rotated counter clockwise to let hydrogen into the regulator. The regulator valve is slowly turned clockwise till hydrogen gas enters the balloon. When a small quantity of hydrogen has entered the balloon, the regulator valve can be closed. The balloon should be double tied to minimise leakage. The cylinder's valve can then be closed and the regulator valve opened to release any trapped hydrogen. The cylinder regulator and key can be removed and the hydrogen cylinder moved back to storage.

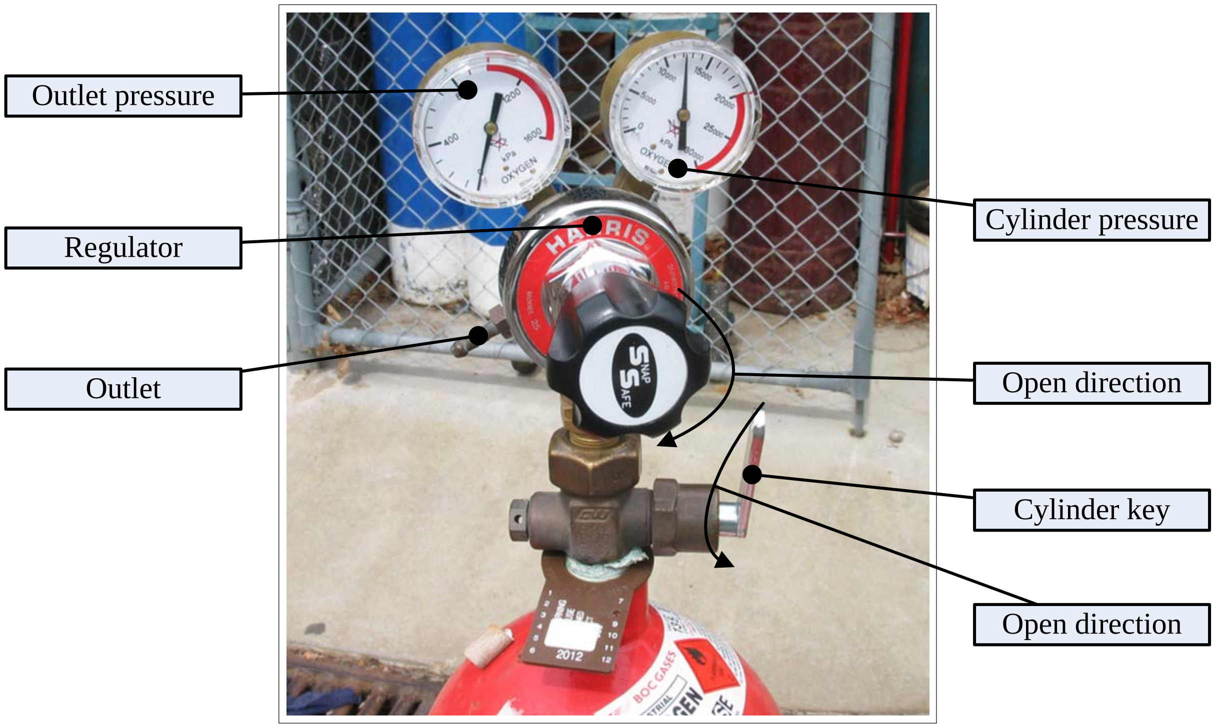


**Figure B.2:** Close up of regulator with valve opening directions

## B.2 Creating a calibration gas mixture

Due to hydrogen being lighter then air, accumulation will occur in ceiling spaces and cavities and can create a severe explosion risk unless adequately vented. Hence the creation of calibration mixture will be conducted in a fume cabinet.

The fume cabinet documented in this procedure is located in the mechanical engineering building, room 1.81 (Figure B.3).

The filled hydrogen balloon must be placed under the fume hood and the fume hood started (Figure B.4).

### B.2.1 Creating the hydrogen and air mixture

Before doing any testing with hydrogen the required materials should be obtained (Figure B.6 and Figure B.5)and the the tester familiarised with the procedure.

#### B.2.1.1 Materials required

**Container** — must have an opening large enough for the sensor. Exact volume must be known, this can be done by filling with water and either measuring the weight or volume.

**Balloons** — preferable helium quality. With the necks removed.


**Figure B.3:** Fume hood located in room 1.81

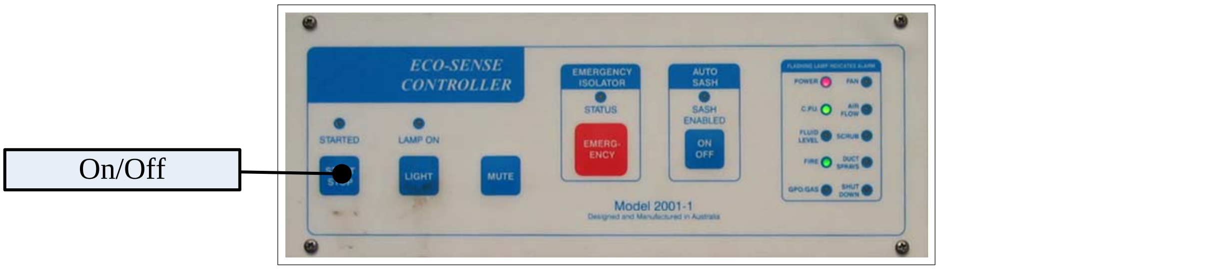


**Figure B.4:** Close up of control panel

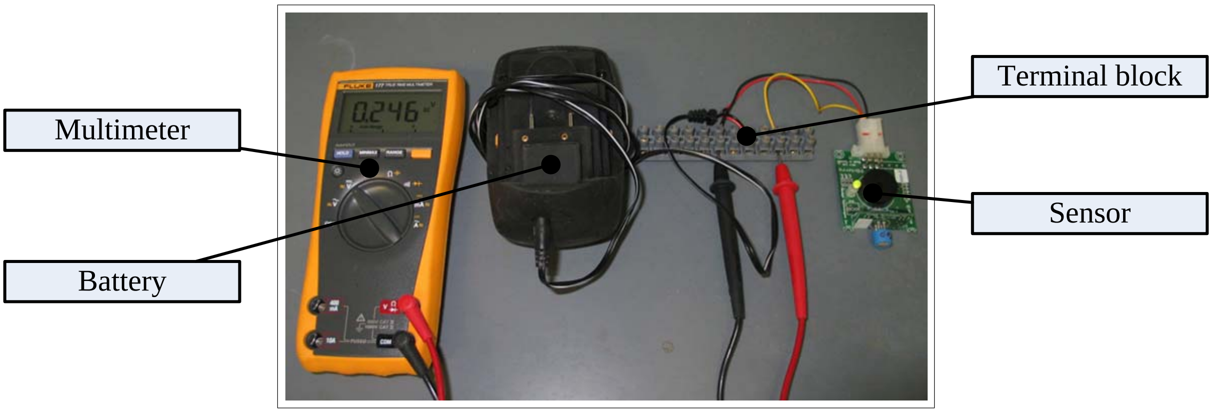


**Figure B.5:** Electrical equipment required for testing procedure

**Syringe with needle** - can be purchased from pharmacy.

**Sensors** — located in the REV room, in box marked hydrogen sensors.

**Battery** — 12 V, a drill battery was used in the example.

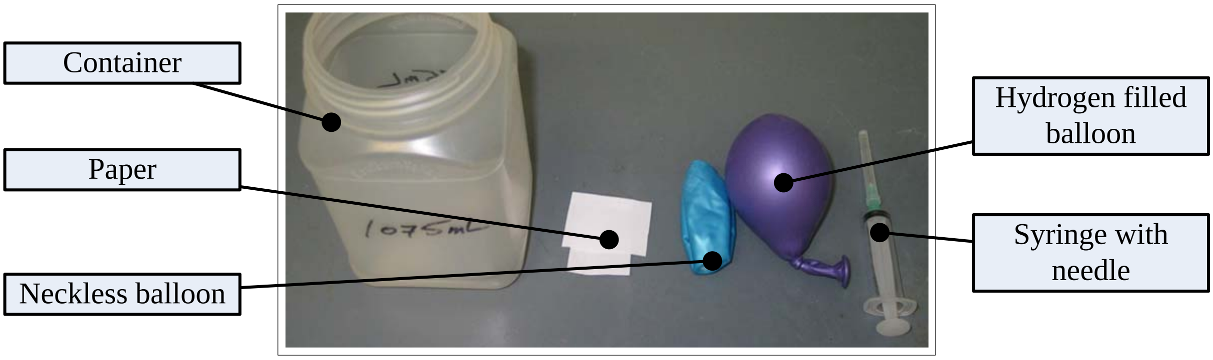


**Figure B.6:** Materials required to perform hydrogen testing

**Terminating block and wire**

**Multimeter** — set on DC voltage.

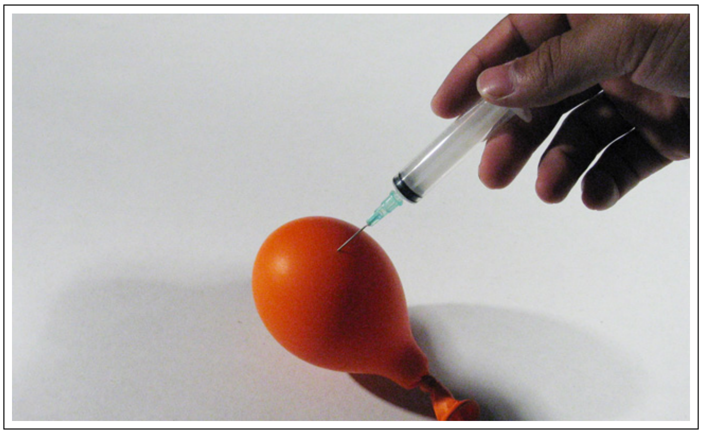

**Figure B.7:** Pure hydrogen gas is drawn into the syringe

**Figure B.8:** The syringe is emptied into the container upside down due to hydrogen's relative density

#### B.2.1.2 Procedure

1. The electrical circuit is setup with all connections secured, in order to prevent sparking.

2. The sensor is placed into the container and the opening covered with the neckless balloon.

3. An empty syringe is inserted into the previously filled balloon and pure hydrogen drawn till the syringe is full (Figure B.7).

4. The full syringe is inserted into the balloon skin covering the opening, and syringe is emptied (Figure B.8).

5. The container will need to be gently shaken to mix the hydrogen and air. This can be helped by placing pieces of paper in the container before shaking.

6. Sensor voltage readings are taken.

When sufficient sensor readings have been recorded, any excess hydrogen gas in the balloons can be released while under the fume hood. The fume hood can be switched off, and it will go into its shut down cycle.

## B.3 Safety checklist

| | ✓ |
|---|---|
| **PRIOR TO TESTING** | |
| Hydrogen testing procedure read | |
| Safety Assessment (Appendix F) read | |
| Personal Protective Equipment obtained | |
| Fume hood room booked | |
| **MATERIALS** | |
| Hydrogen cylinder | |
| Cylinder attachments (trolley, key and regulator) | |
| Balloons (helium quality) | |
| Container of known volume | |
| Syringe with needle | |
| Hydrogen concentration sensors | |
| Battery (12–48 V) | |
| Terminating block and wire | |
| Multimeter | |
| **OBTAINING A QUANTITY OF HYDROGEN** | |
| PPE worn (safety glasses) | |
| All ignition sources eliminated | |
| Cylinder moved away from cage with trolley | |
| Regulator screwed onto cylinder | |
| Cylinder valve opened | |
| Balloon slightly filled | |
| **CREATING A CALIBRATION GAS MIXTURE** | |
| PPE worn (safety glasses) | |
| Filled balloons placed under running fume hood | |
| Electrical circuit constructed | |
| Sensor placed into container and covered with neckless balloon | |
| Empty syringe filled with pure hydrogen drawn | |
| Syringe emptied into container | |
| Container gently shaken | |
| Sensor voltage readings measured | |
| Unused hydrogen released | |

Signed____________________ Date____________________

# Appendix C

# Hydrogen concentration sensor test results

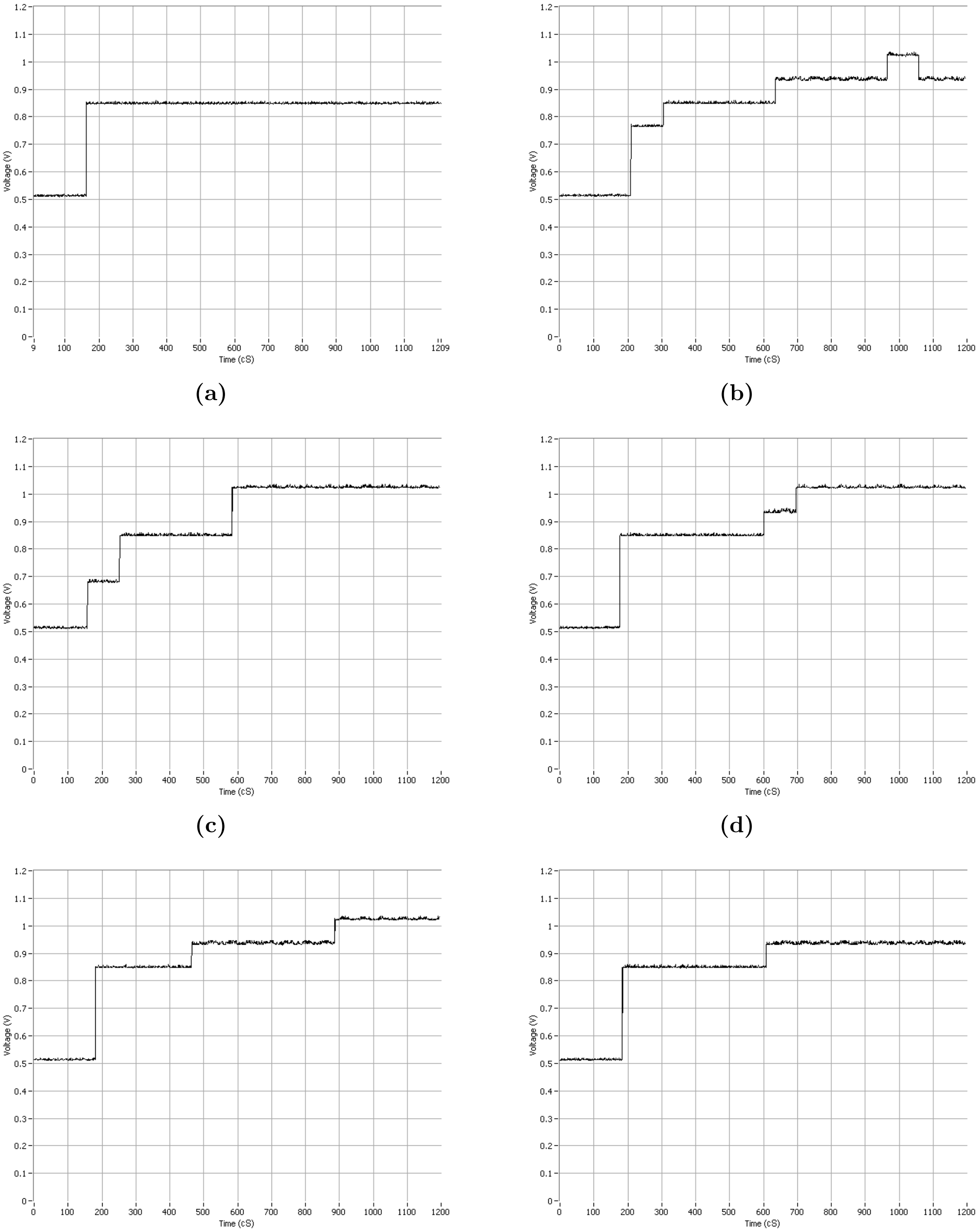


(a) (b) (c) (d) (e) (f)

**Figure C.1:** Calibration test results from MiniKnowz.

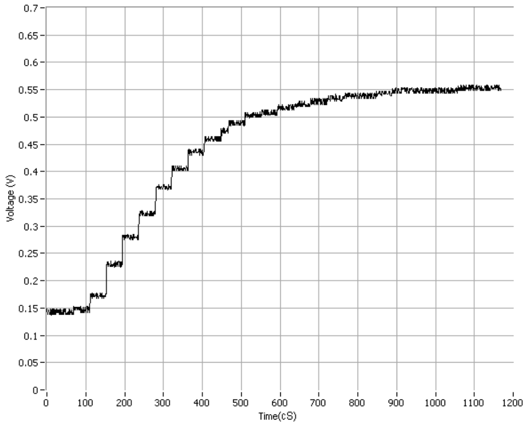


**(a)**

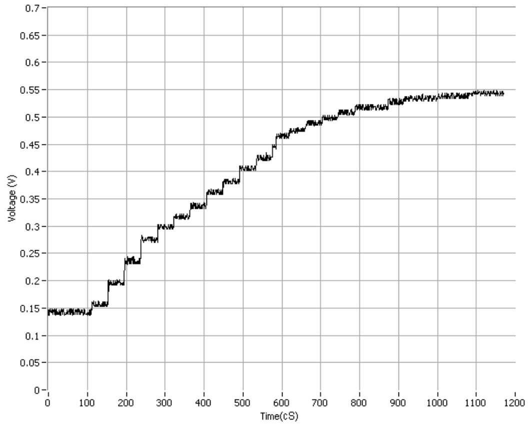


**(b)**

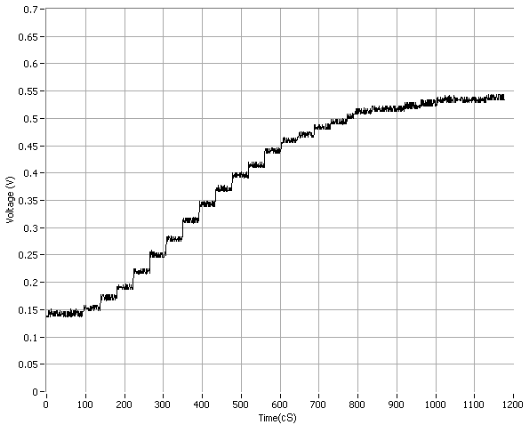


**(c)**

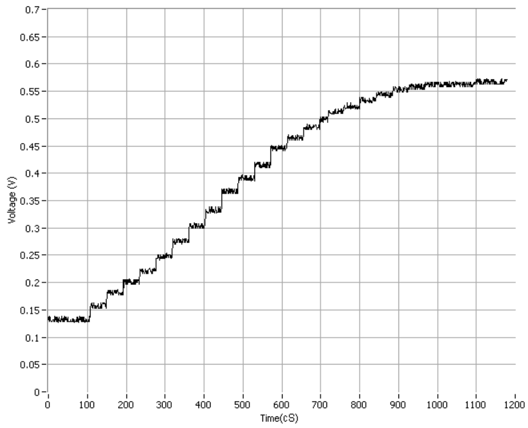


**(d)**

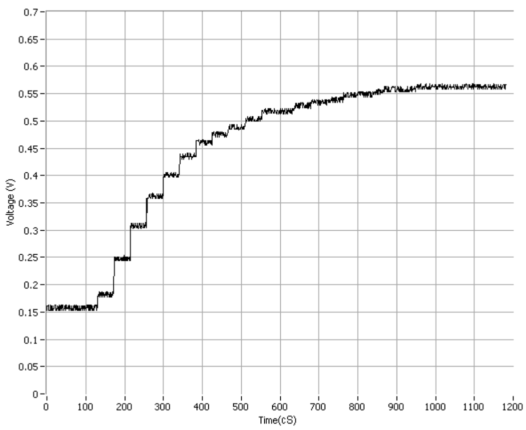


**(e)**

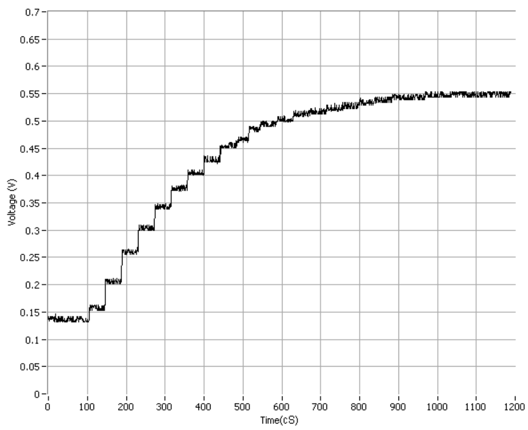


**(f)**

**Figure C.2:** Calibration test results from Panterra-CAT.

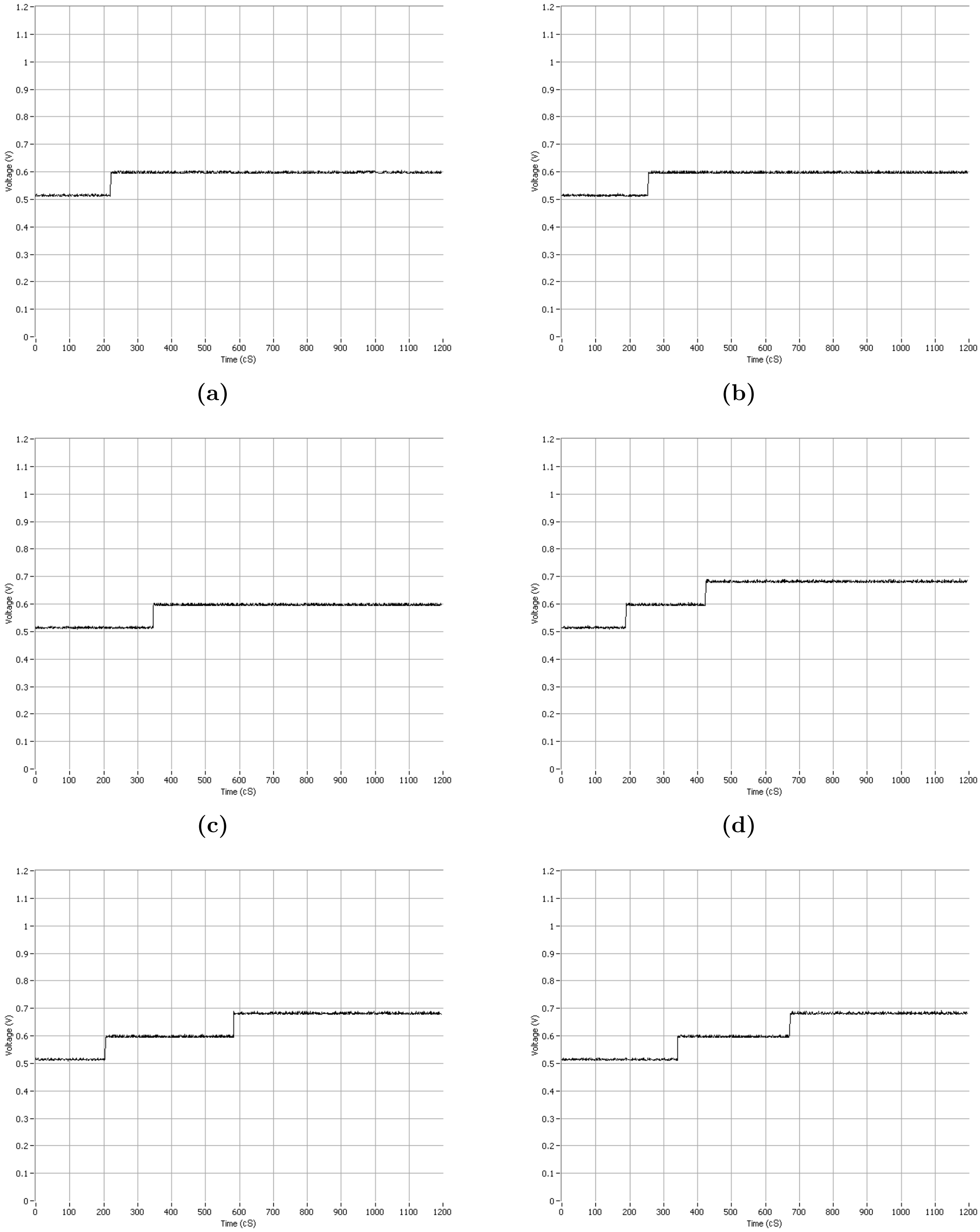


(a) (b) (c) (d) (e) (f)

**Figure C.3:** Interference gas test results from MiniKnowz.

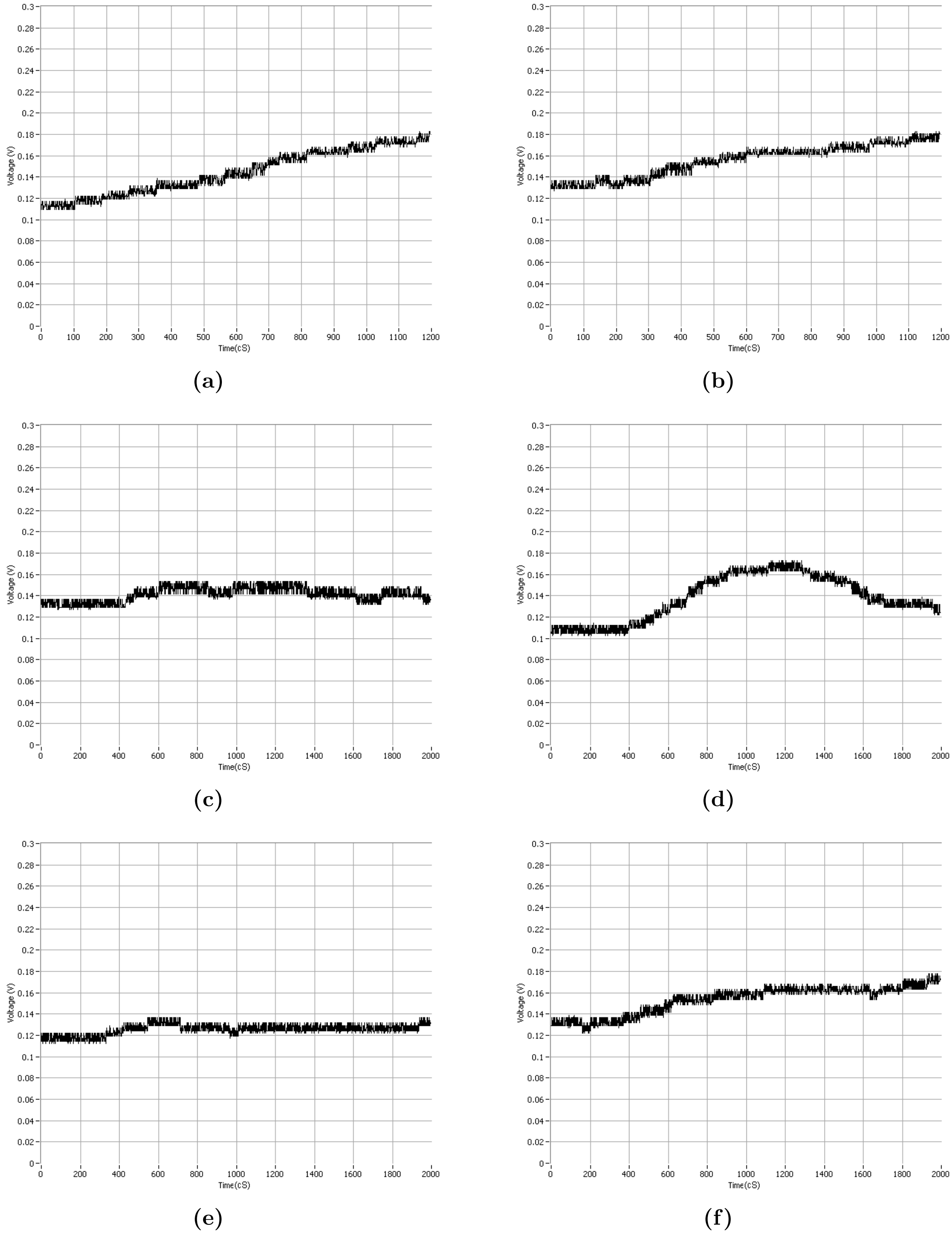


**Figure C.4:** Interference gas test results from Panterra-CAT.

# Appendix D

# Test equipment

The following equipment was used to either create a know electrical quantity or to measure electrical measurements.

## D.1 Power supply

The power source that was used for the sensor testing, was a dual channel lab power supply capable of outputting 0–30 V with a maximum current rating of 5 A. It was useful for testing the voltage and current sensors which required a varied voltage in ($V_{in}$) and to also produce 12 V for the dual polarity power supply. If a precise voltage was required a digital multimeter was used, rather than the analogue needles.

In order to determine how 'clean' the power supply was, the output was observed with an oscilloscope (Figure D.1)

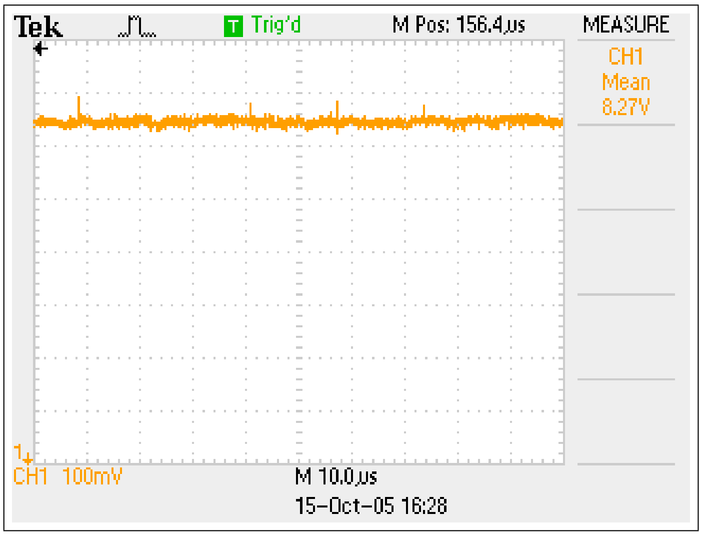


**Figure D.1:** Power supply output viewed with oscilloscope

## D.2 Data acquisition hardware

The DAQ hardware used for the majority of testing was the USB-1208FS from Measurement Computing Corporation [40] (Figure D.2). The DAQ hardware specifications of concern are in Table D.1, Table D.2 and Table D.3.


**Figure D.2:** The DAQ hardware used for the majority of testing

**Table D.1:** DAQ general specifications

| Parameter | Specification |
|---|---|
| Maximum input voltage | ±28 V max |
| Throughput software paced | 250 S/s typical |
| Resolution | 12 bits |

**Table D.2:** DAQ accuracy at different voltage ranges

| Range (V) | Accuracy (LSB) | Accuracy at full scale (mV) |
|---|---|---|
| ±20 | 5.1 | 49.766 |
| ±10 | 6.1 | 29.766 |
| ±5 | 8.1 | 19.766 |

**Table D.3:** DAQ noise at different voltage ranges

| Range (V) | $LSB_{rms}$ |
|---|---|
| ±20 | 0.30 |
| ±10 | 0.30 |
| ±5 | 0.45 |

Tests involving the DAQ hardware, were always set on the minimum needed voltage range i.e. a sensor outputting a voltage of 0–5 V was set on the range ±5 V, 0–15 V required for a voltage sensor was set on the range ±20 V.

## D.3 Multimeter

A multimeter was used to measure currents, voltages and resistances. The multimeter used was the Fluke 170 Series True-RMS Digital Multimeter. The multimeter's specifications of concern are in Table D.4.

**Table D.4:** Multimeter specifications

| Function | Resolution | Accuracy (±[% of Reading] + [Counts]) |
|---|---|---|
| DC voltage | 0.001 V | 0.09 % + 2 |
| DC current | 0.001 A | 1.0 % + 3 |
| Resistance | 0.1 Ω | 0.9 % + 2 |

# Appendix E

# Current shunt test results

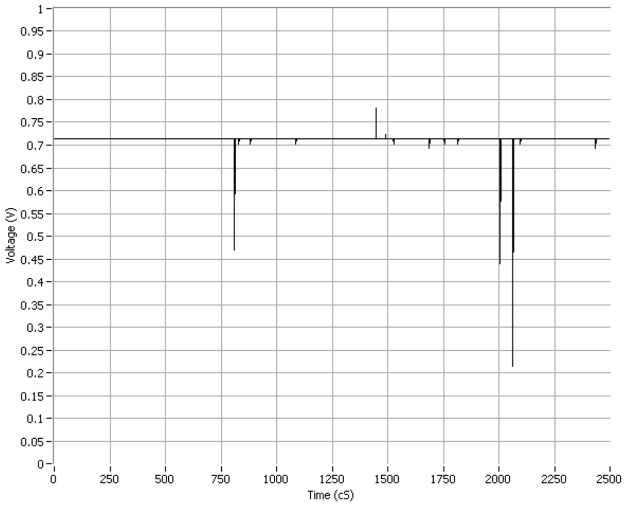


**Figure E.1:** 50 mm current shunt test with updated current sensor

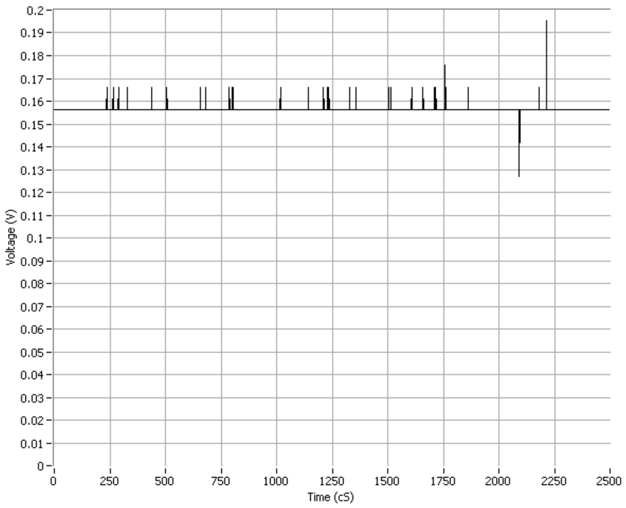


**Figure E.2:** 200 mm current shunt test with updated current sensor

Table E.1: Current shunt test using 50 mm of shielded cable

| Actual current (A) | Measured voltage (V) |
|---|---|
| 0.11±0.0041 | 0.0292969 |
| 0.42±0.0072 | 0.107422 |
| 0.8±0.011 | 0.205078 |
| 1.27±0.0157 | 0.322266 |
| 1.7±0.02 | 0.429687 |
| 1.96±0.0226 | 0.488281 |
| 2.34±0.0264 | 0.585937 |
| 2.58±0.0288 | 0.644531 |
| 2.95±0.0325 | 0.732422 |
| 3.29±0.0359 | 0.820312 |

Table E.2: Current shunt test using 200 mm of non-shielded cable

| Actual current (A) | Measured voltage (V) |
|---|---|
| 0.05±0.0035 | 0 |
| 0.38±0.0068 | 0.0195312 |
| 0.61±0.0091 | 0.0292969 |
| 0.74±0.0104 | 0.0390625 |
| 0.99±0.0129 | 0.0488281 |
| 1.07±0.0137 | 0.058937 |
| 1.29±0.0159 | 0.068594 |
| 1.47±0.0177 | 0.0683594 |
| 1.65±0.0195 | 0.078125 |
| 1.92±0.0222 | 0.0878906 |
| 2.16±0.0246 | 0.107422 |
| 2.31±0.0261 | 0.117187 |
| 2.56±0.0286 | 0.126953 |
| 2.97±0.0327 | 0.146484 |
| 3.29±0.0359 | 0.15625 |

# Appendix F

# STUDENT FINAL YEAR PROJECT - SAFETY ASSESSMENT

## F.1 PROJECT OUTLINE

Project title 'Sensors for the Renewable Energy Vehicle' conducted by Travis Hydzik, supervisor Associate Professor James Trevelyan.

The requirement of the project is to calibrate a Neodym Technologies hydrogen sensor according to the organisation's recommended calibration procedure. The frequency of calibration is as often as practical and no less than once every six months.

The calibration procedure requires generating a calibration gas mixture of hydrogen and air in a leak free container of fixed volume.

It is proposed to collect the hydrogen gas from the storage cylinder into a small rubber balloon (partially inflated). This part of the operation would be carried out in a well ventilated location, outside the building. The mixing and calibration part of the operation would be carried out in a laboratory fume cabinet.

Since the volume of hydrogen gas is small and the air/gas concentration very low, below 0.5 % and well below the explosive range of hydrogen, the School is permitting this work to be carried out in a laboratory fume cabinet. The short duration and infrequent calibration intervals have also been considered in making this decision.

In addition, the proposed calibration method and gas quantities and concentrations involved have been discussed with Dr. Allan McKinley from the School of Chemistry, who advises that the proposed method is satisfactory.

## F.2 DESCRIPTION OF EXPERIMENTAL PROCEDURE

A small balloon will be filled with hydrogen from the storage cylinder and tied off. This operation is conducted outside the building.

The remaining operations are conducted in the laboratory fume cabinet.

The sensor will be placed in a 1075 ml clean container of air with the opening covered by a second balloon with the neck removed. An empty syringe is inserted into the balloon containing hydrogen and 5 cc of gas is drawn off into the syringe. The contents of the syringe are then transferred into the container, through the second balloon membrane. The container is then gently shaken to mix the hydrogen and air.

Sensor calibration is then carried out. The test is of approximately 15 minutes duration.

## F.3 TASK HAZARD IDENTIFICATION

The proposed calibration routine has been reviewed and the following potential safety hazards have been identified:

1. **Handling and Use of Hydrogen Gas** - hydrogen has a wide combustible range when mixed with air (approximately 4 to 80 %). In addition, it is lighter than air and will accumulate in ceiling spaces and cavities and create a severe explosion risk unless adequately ventilated.

2. **Ignition Sources** - potential ignition sources include flames such as cigarettes, and matches or even sparks generated by electrical devices or static electricity.

3. **General Laboratory Hazards** - working in a chemical laboratory may expose an untrained person to other diverse hazards.

## F.4 SAFETY CONTROL MEASURES

The Task Hazard Identification indicated the principle hazard associated with this project is the use of hydrogen. The magnitude of this risk is decreased in the latter stages of the calibration task, by the low hydrogen/air concentration that is outside the specified explosive range.

The most hazardous part of the procedure involves the use of the hydrogen storage cylinder and the mixing procedure, given that the hydrogen concentration may not be precise, since volume will vary with balloon pressure. There is the requirement to exercise great care and ensure that there is no opportunity for gas accumulation or ignition sources to be present.

1. **MSDS** - A copy of the MSDS for hydrogen must be available and all individuals involved in handling hydrogen gas must be familiar with its contents.

2. **Handling and Use of Hydrogen Gas** - The hydrogen cylinder must be stored and used outside the building. Collection of hydrogen from the cylinder should involve two people assisting in the operation. This part of the operation should be carried out when the area is quiet and no ignition sources are present.

3. **Mixing Hydrogen and Air** - This must be conducted in a fume cabinet, free from potential ignition sources or other flammable or corrosive substances stored in the fume cabinet at the same time.

4. **Safety Signs** - Since the preparation and measurement phase are of short duration, ensure that only authorised personnel are present in the laboratory at the time. A Hazard No Entry sign should be displayed on the laboratory door to restrict other people from entering.

5. **Personal Protective Equipment** - It is recommended that safety glasses are worn through the task including use of the fume cabinet sash screen as an additional safety screen whenever possible. Enclosed footwear is a requirement for all laboratories.

6. **On Completion** - Ensure that accumulations of hydrogen are removed from all test apparatus.

7. **Working Alone** - Since there are some potential hazards associated with this operation, this work should not be attempted outside of normal working hours.

## F.5 MEDICAL SURVEILLANCE AND PERMITS

Not applicable.

## F.6 EXPOSURE LIMIT

Not applicable.

## F.7 ADVERSE HEALTH EFFECTS

Not applicable.

## F.8 PRINCIPLE HAZARDS

Possible explosive gas mixture.

## F.9 EMERGENCY PROCEDURES

In the case of injury contact School First Aid Officers or UWA Emergency Services on 2222 if the damage extends to property damage and serious injury. Note the position of the nearest suitable fire extinguisher in case it is needed.

*Safety Assessment conducted by Rob Greenhalgh, School of Mechanical Engineering Safety Officer, on 18th August 2005.*

*Acknowledgment and thanks to Dr Allan McKinley (School of Chemistry) for his advice in addressing safety issue with hydrogen.*

# Appendix G

# Electrical block diagram

The following block diagram gives a indication of the required electrical measurements in the REV's electrical system.

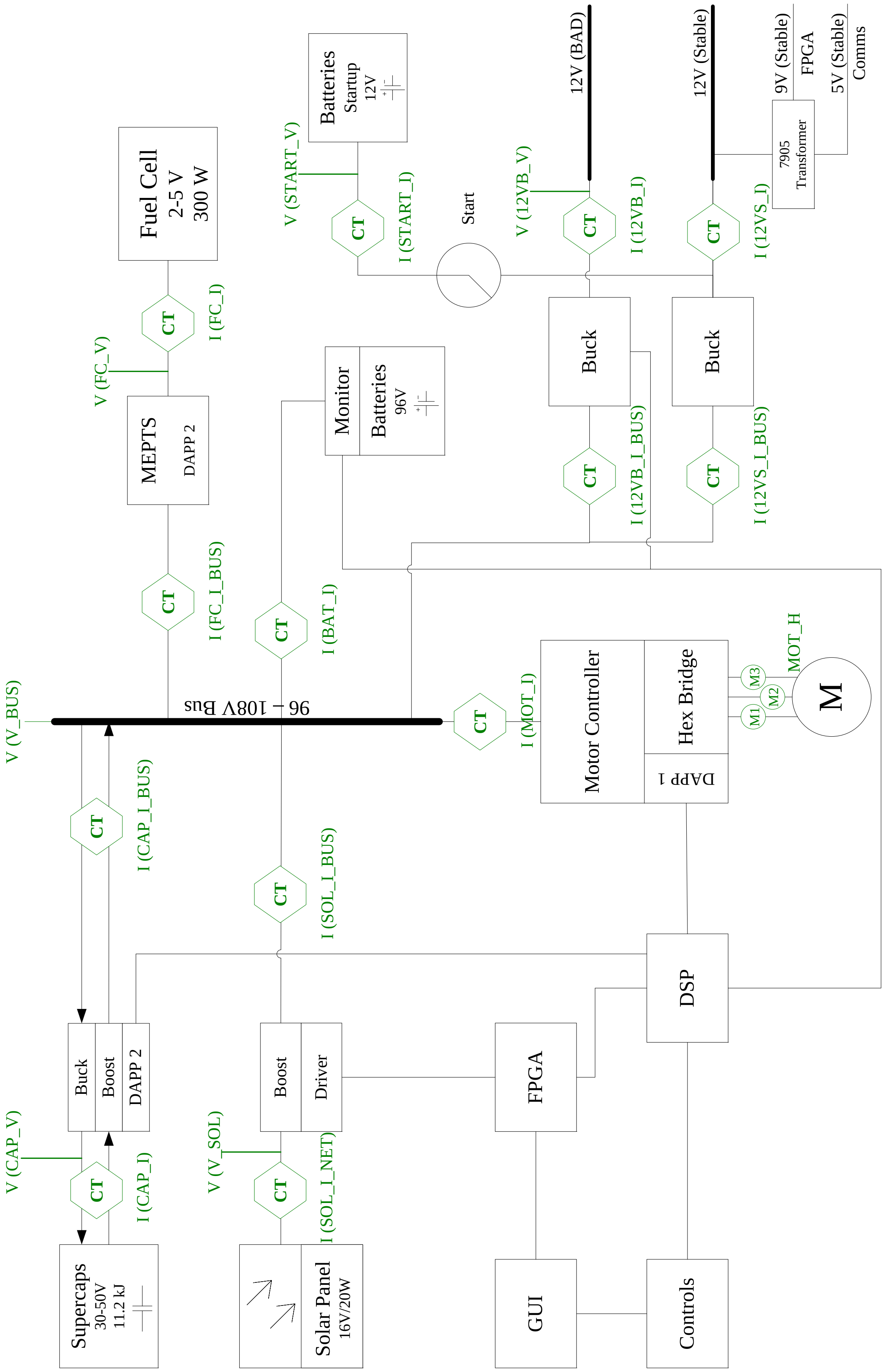
Fuel Cell
2-5 V
300 W
MEPTS
DAPP 2
V (FC_V)
I (FC_I)
I (FC_I_BUS)
Batteries
Startup
12V
V (START_V)
I (START_I)
Start
Monitor
Batteries
96V
I (BAT_I)
12V (BAD)
12V (Stable)
V (12VB_V)
I (12VB_I)
I (12VS_I)
Buck
Buck
I (12VB_I_BUS)
I (12VS_I_BUS)
7905
Transformer
9V (Stable)
FPGA
5V (Stable)
Comms
96 – 108V Bus
V (V_BUS)
I (MOT_I)
Motor Controller
Hex Bridge
DAPP 1
M1
M2
M3
MOT_H
M
I (CAP_I_BUS)
I (SOL_I_BUS)
Buck
Boost
DAPP 2
Boost
Driver
FPGA
DSP
V (CAP_V)
I (CAP_I)
V (V_SOL)
I (SOL_I_NET)
Supercaps
30-50V
11.2 kJ
Solar Panel
16V/20W
GUI
Controls
CT